Monthly Notices
of the
ROYAL ASTRONOMICAL SOCIETY

MNRAS **446,** 391–410 (2015) doi:10.1093/mnras/stu2105

Long-term photometric behaviour of outbursting AM CVn systems

David Levitan,[1]★ Paul J. Groot,[1,2] Thomas A. Prince,[1] Shrinivas R. Kulkarni,[1] Russ Laher,[3] Eran O. Ofek,[4] Branimir Sesar[1] and Jason Surace[3]

[1]*Division of Physics, Mathematics, and Astronomy, California Institute of Technology, Pasadena, CA 91125, USA*
[2]*Department of Astrophysics/IMAPP, Radboud University Nijmegen, PO Box 9010, NL-6500 GL Nijmegen, the Netherlands*
[3]*Spitzer Science Center, MS 314-6, California Institute of Technology, Pasadena, CA 91125, USA*
[4]*Benoziyo Center for Astrophysics, Weizmann Institute of Science, 76100 Rehovot, Israel*

Accepted 2014 October 8. Received 2014 October 7; in original form 2014 July 15

ABSTRACT

The AM CVn systems are a class of He-rich, post-period minimum, semidetached, ultra-compact binaries. Their long-term light curves have been poorly understood due to the few systems known and the long (hundreds of days) recurrence times between outbursts. We present combined photometric light curves from the Lincoln Near Earth Asteroid Research, Catalina Real-Time Transient Survey, and Palomar Transient Factory synoptic surveys to study the photometric variability of these systems over an almost 10 yr period. These light curves provide a much clearer picture of the outburst phenomena that these systems undergo. We characterize the photometric behaviour of most known outbursting AM CVn systems and establish a relation between their outburst properties and the systems' orbital periods. We also explore why some systems have only shown a single outburst so far and expand the previously accepted phenomenological states of AM CVn systems. We conclude that the outbursts of these systems show evolution with respect to the orbital period, which can likely be attributed to the decreasing mass transfer rate with increasing period. Finally, we consider the number of AM CVn systems that should be present in modelled synoptic surveys.

Key words: accretion, accretion discs – surveys – binaries: close – novae, cataclysmic variables – white dwarfs.

1 INTRODUCTION

The AM CVn systems are a rare class of ultracompact, post-period minimum, stellar binaries with some of the smallest orbital separations known. Ranging in orbital period from 5 to 65 min, they are believed to be composed of a white dwarf accreting from a lower mass white dwarf or semidegenerate helium star donor (Paczyński 1967; Faulkner, Flannery & Warner 1972). We refer the reader to Nelemans (2005) and Solheim (2010) for reviews.

As a result of their mass-transferring nature, most AM CVn systems show inherent photometric variability on multiple time-scales, believed to be largely dependent on the orbital period and mass transfer rate of the particular system. The phenomenological behaviour of AM CVn systems has been separated into two states – a 'high' state corresponding to high rates of mass transfer resulting in an optically thick accretion disc around the primary – and a 'quiescent' state corresponding to low rates of mass transfer and an optically thin disc. The high state is generally associated with those systems having orbital periods <20 min and the quiescent state with those having orbital periods >40 min. High state systems exhibit superhump behaviour like that found in some cataclysmic variables (CVs; Warner 1995) with photometric variability close to the orbital time-scale at an amplitude of $\approx$0.1 mag (e.g. Patterson et al. 2002).

Systems with orbital periods between $\approx$20 and $\approx$40 min have been observed to alternate between the high and quiescent states and have behaviour similar to that of superoutbursts in dwarf novae and are thus called 'outbursting' AM CVn systems (e.g. Ramsay et al. 2012). In outburst, these systems are typically 3–5 mag brighter than in quiescence and these outbursts have been observed to recur on time-scales from $\sim$40 d to several years. Some systems, particularly those at the short-period end, are also observed to have shorter, 'normal' outbursts that last 1–1.5 d and are typically seen 3–4 times between the longer 'super'-outbursts (e.g. Kato et al. 2000; Levitan et al. 2011). Given the much longer cadences for the data presented here, we are interested only in superoutbursts and will refer to them as just outbursts, unless explicitly specified.

One of the outstanding questions about AM CVn systems is the disagreement between population density estimates derived from population synthesis modelling and those calculated from the number of observed systems (see e.g. Carter et al. 2013 for the latest overview). The intrinsic low luminosity of the systems means few systems have been discovered; the known sample remained under a

★ E-mail: dlevitan@astro.caltech.edu

dozen for almost 40 years until the availability of the Sloan Digital Sky Survey (SDSS). This also makes obtaining a systematically identified sample of AM CVn systems large enough to measure the population density difficult. The recent availability of large-area surveys has allowed for the identification of AM CVn systems both from their spectra (or colours) and their aforementioned light curves in a systematic fashion, with relatively well-understood selection biases. This has led to the number of known AM CVn systems tripling in the last decade and the identification of two complementary, systematically selected sets of systems.

Searches of the SDSS spectroscopic data base for He-rich, H-poor sources have been particularly successful, with nine new systems identified (Anderson et al. 2005, 2008; Roelofs et al. 2005; Carter et al. 2014b). Roelofs, Nelemans & Groot (2007b) found that the spectroscopic completeness of the SDSS data base in the relatively sparse region of colour–colour space that AM CVn systems are believed to occupy, and at the faint apparent magnitudes where most systems are expected to be found, was only ∼20 per cent. A subsequent effort using the SDSS imaging data to conduct a targeted spectroscopic survey identified seven additional systems (Roelofs et al. 2009; Rau et al. 2010; Carter et al. 2013).

More recently, a significant number of AM CVn systems has been found from their photometric variability using large-area synoptic surveys. In particular, the Palomar Transient Factory (PTF) has systematically identified seven new AM CVn systems from their photometric outbursts in a colour-independent manner (Levitan et al. 2011, 2013, 2014) as well as over 80 new CVs. Three AM CVn systems have also been identified in a less systematic fashion from the Catalina Real-Time Transient Survey (CRTS; Woudt, Warner & Motsoaledi 2013; Breedt et al. 2014). We note that photometric surveys are only sensitive to the shorter period outbursting systems, while spectroscopic surveys are most sensitive to longer period systems, which have stronger emission lines.

Despite the significant increase in the known sample, the population density question remains to be fully answered. Roelofs et al. (2007b) used the original SDSS sample of AM CVn systems to show that the population synthesis estimate by Nelemans et al. (2001) was high by an order of magnitude. The re-calibrated population density was used to predict that 40 new systems would be discovered by the follow-up project (Roelofs et al. 2009). Instead, this search yielded only seven new systems, implying that the original population estimates were a factor of 50 too high (Carter et al. 2013). No explanation for this difference has been given in the literature.

The PTF's search for AM CVn systems has provided a second set of systematically identified systems, determined without the use of colour selection, to verify current population models. However, in order to draw any conclusions on the population of AM CVn systems from an outburst search, the outburst phenomena itself needs to be better understood. It is believed that the outburst mechanism in AM CVn systems can be described by adjustments to the same disc instability model (DIM) as that used to model the outbursts of CVs (see e.g. Lasota 2001 for an excellent review). Recent work has, in fact, shown that the outburst in AM CVn systems can be modelled using the DIM (Tsugawa & Osaki 1997; Kotko et al. 2012), although the changes in outburst patterns for AM CVn systems (e.g. CR Boo; Kato et al. 2000, 2001) are not yet explained.

Efforts to understand outbursts based on observations have been hampered by the lack of long-term light curves for most AM CVn systems. Ramsay et al. (2012), hereafter R12, have performed the most substantial work in this area. They used the Liverpool Telescope to monitor 16 AM CVn systems for 2.5 yr. However, the use of dedicated observations provided only a short baseline, and even several known outbursting systems were not detected in outburst during their monitoring. Only a few systems have been monitored for more than a few years (most notably CR Boo; Honeycutt et al. 2013), but the variety of outbursts, as we describe in this paper, requires data for more than one system.

Earlier work on individual systems has provided some information on their outburst recurrence times. Both Levitan et al. (2011), hereafter L11, and R12 differentiated between shorter orbital-period systems (20 min $< P_{\rm orb} <$ 27 min) and longer orbital-period systems (27 min $< P_{\rm orb} <$ 40 min). They noted that the former of these groups has fairly well-established recurrence times of less than a few months while the latter group has either very poorly determined recurrence times or no determined recurrence time.

Here, we extend the work of R12 by using three separate synoptic surveys to extend our baseline to almost 10 yr for many systems. This allows us, for the first time, to consider the outburst frequency of those systems outbursting only once every several years. Additionally, since we use non-dedicated observations from large-area surveys, we are able to analyse recently discovered AM CVn systems by drawing on past data for these systems. We do note that a significant disadvantage of synoptic surveys is the often erratic coverage and the long cadences.

This paper is organized as follows. We begin by describing the surveys, data processing, and analysis methods in Section 2. We review the known outbursting AM CVn systems in Section 3 and present our composite light curves, along with initial analysis of the outbursts. In Section 4, we discuss AM CVn system evolution, outburst properties, and make predictions on the observed number of systems in current synoptic surveys. We summarize our conclusions in Section 5.

2 OBSERVATIONS AND REDUCTION

2.1 Data sources

The observations presented in this paper come from three synoptic surveys: the PTF, the CRTS, and the Lincoln Near Earth Asteroid Research (LINEAR) survey. In the remainder of this section, we summarize each of these surveys, including an overview of the survey parameters, details of data processing, and a discussion of the limiting magnitudes presented here for the survey. The limiting magnitudes are particularly important for this project, as most known outbursting AM CVn systems are extremely faint in quiescence.

2.1.1 Palomar transient factory

The PTF[1] (Law et al. 2009; Rau et al. 2009) used the Palomar 48″ Samuel Oschin Schmidt Telescope to image 7.3 deg^2 of the sky simultaneously using 11 2048 × 4096 pixel CCDs. The typical PTF cadence of 1–5 d was primarily chosen to discover supernovae. Certain areas of the sky have been observed with a higher cadence – from 1 d down to 10 min. Typically, two individual exposures separated by 30 min are taken every day to eliminate asteroids and artefacts. The PTF observes in either R band or g' band, with an Hα survey during full moon. The 5σ limiting magnitude of the survey is $R \sim 20.6$ and $g' \sim 21.0$ with saturation around 14th magnitude. The PTF data are the best calibrated and deepest of the large-area

[1] http://www.ptf.caltech.edu/

synoptic surveys used here. However, it is also the youngest and has the least amount of data.

The PTF data are processed through the so-called photometric pipeline which uses aperture photometry and prioritizes photometric accuracy over processing speed (Laher et al. 2014). After de-biasing and flat-fielding, catalogues are generated using SExtractor (Bertin & Arnouts 1996). Photometric calibration relative to SDSS fields observed in the same night provides an absolute calibration accuracy of better than ∼2–3 per cent on photometric nights, but this can be significantly inaccurate on nights with changing weather conditions (Ofek et al. 2012). Relative photometric calibration is able to correct for such changes as well as improve the precision of photometry at the bright end to 6–8 mmag and at the faint end to ∼0.2 mag. The basic approach of the algorithm is described in Ofek et al. (2011) and L11 with PTF-specific details to be published at a future time. Although this algorithm is primarily a relative calibration algorithm, it simultaneously uses external calibration references to provide an absolute calibration. For the PTF data, we use the median value of the absolute-calibrated photometric measurements.

The photometric pipeline produces two limiting magnitude estimates for each exposure as part of the calibration process. The first estimate defines the limiting magnitude as the magnitude at which 95 per cent of sources in a deep co-added image are present in an individual exposure. The second estimate is a theoretical estimate of the maximum magnitude at which a 5σ detection is possible. Typically, this 5σ detection limit is reached ∼0.5 mag fainter than the 95 per cent limiting magnitude estimate, but we have found it to be unreliable in poor weather conditions, in part because it relies on the zero-points calculated from the comparison to SDSS, which themselves are unreliable in poor weather. Here, we use the former estimate due to its more consistent performance.

2.1.2 *Catalina Real-Time Transient Survey*

The CRTS[2] (Drake et al. 2009) uses three separate telescopes: the Catalina Sky Survey 0.7 m Schmidt (CSS), the Mount Lemmon Survey 1.5 m (MLS), and the Siding Spring Survey 0.5 m Schmidt (SSS). The fields of view are, respectively, 8.1 $\deg^2$, 1.2 $\deg^2$, and 4.2 $\deg^2$, with corresponding limiting magnitudes in V of 19.5, 21.5, and 19.0. The majority of data currently available is from the CSS, and has a typical cadence of one set of four exposures per night per field separated by 10 min, repeated every two weeks.

The CRTS DR2 public release provides both the ability to see all exposures covering a given part of the sky and the ability to download light curves around a set of coordinates. We began by downloading the list of exposures at each location, as well as the light curve for the target, from the 'photcat' catalogue. This catalogue is the set of sources identified in deep co-added CRTS images, as part of the CRTS pipeline. We retained only those exposures with 1 arcsec < full width at half-maximum < 4 arcsec and exposure times between 1 and 120 s to eliminate problematic exposures. We downloaded light curves of all objects within ∼0.3 $\deg^2$ of the centre of the CRTS pointing for these exposures.

Although we would prefer to estimate the limiting magnitude with the same method as that used for PTF exposures, the lack of publicly available deep co-added images from the CRTS precludes this. We thus estimate the 5σ limiting magnitude of each exposure to be the faintest star detected in this set of light curves. We then subtract 0.5 mag from this limiting magnitude to convert this into a '95 per cent limiting magnitude', as defined for the PTF (i.e. $m_{\rm lim} = m$(faintest star) − 0.5). These estimates are typically consistent with the average limiting magnitudes of the CRTS (Drake et al. 2009).

A few of the AM CVn systems observed by the CRTS are too faint to be detected in the default 'photcat' catalogue. Detections not associated with this set of sources are in the 'orphancat' catalogue (Drake, private communication). In these cases, we assumed that any detection in the 'orphancat' within 3.5 arcsec (∼1.5 × the pixel scale of the CSS, similar to criteria used for PTF source association) of the target coordinates was a detection of our target.

2.1.3 *Lincoln Near Earth Asteroid Research survey*

The LINEAR survey[3] (Stokes et al. 2000) used two telescopes at the White Sands Missile Range for a synoptic survey primarily targeted at the discovery of near-Earth objects. Sesar et al. (2011) re-calibrated the LINEAR data using the SDSS survey, resulting in ∼200 unfiltered observations per object (∼600 observations for objects within ±10° off the Ecliptic plane) for 25 million objects in the ∼9000 $\deg^2$ of sky where the LINEAR and SDSS surveys overlap (roughly, the SDSS Galactic cap north of Galactic latitude 30° and the SDSS Stripe 82 region). Each exposure covered ∼2 $\deg^2$ to a 5σ limiting magnitude of $r' \sim 18$, as determined by the calibration of the unfiltered exposures to the SDSS survey. The photometric precision of LINEAR photometry is ∼0.03 mag at the bright end ($r' \sim 14$) and ∼0.2 mag at $r' = 18$ mag.

The published LINEAR data set contains information only on source detections, and provides no list of exposures for a particular field. We thus need to both determine when the target was observed, as well as the limiting magnitudes of those exposures. To identify exposures on which a particular target was not detected we downloaded light curves for all sources within 20 arcmin of the target. We assumed that a single MJD corresponded to a single exposure and identified those sources for which there were detections for at least 90 per cent of the MJDs at which the target was detected. Lastly, we identified all MJDs when this group of sources was detected and thus found the non-detections of the target by comparing this list to the list of target detections.

To estimate limiting magnitudes when the target was not detected, we used a similar technique as we did with the CRTS data. Since the centre of the frame coordinates is not available, we used only those stars earlier identified to be near the target. We estimate the 95 per cent limiting magnitudes to be 0.5 mag brighter than the faintest star observed for each exposure.

2.1.4 *Palomar 60″ data*

Some data for CR Boo were obtained using targeted observations with the Palomar 60″ (P60) telescope. This data were de-biased, flat-fielded, and astrometrically calibrated with the P60 Automated Pipeline (Cenko et al. 2006). Photometric measurements were made using the Starlink package AUTOPHOTOM and calibrated using the relative photometric algorithm described in L11. The absolute scale was tied to the SDSS DR9 catalogue (Ahn et al. 2012).

[2] http://crts.caltech.edu/

[3] Public access to LINEAR data is provided through the SkyDOT website (https://astroweb.lanl.gov/lineardb/).

2.1.5 *Photometric data calibration*

Although we use data from three different surveys, we decided to avoid jointly calibrating the light curves. The primary reason for this decision is that the wide-field nature of the surveys requires a large number of calibration sources. With the PTF photometric pipeline, we use 350–400 stars to calibrate light curves for each $\sim$0.7 deg^2 section of the sky (that falling on one detector). Given our lack of access to the raw CRTS and LINEAR data sets, it would be difficult to find these many calibration sources for each target. Although it is possible to calibrate with fewer stars, the lack of filters for the CRTS and LINEAR surveys makes this calibration more difficult, since we would need to account for different CCD response curves, the presence of filters, and source colours. Regardless, our primary interest is in large-scale photometric variability relative to a quiescent magnitude, and even a systematic offset of several tenths of a magnitude between surveys is acceptable.

2.2 Outburst definitions

Although outbursts are often easy to identify by eye, a quantitative definition is necessary for a systematic study. We define an outburst to be $\geq$2 detections that are brighter than the quiescent magnitude by the greater of 0.5 or 3σ mag, where σ is the scatter of the light curve while the system is in quiescence. At least two of the detections must be within 15 d. While the light curve of the system satisfies both conditions, we consider it to be in outburst. The quiescent magnitude is taken to be the median of the light curve or, for the faintest systems, from the literature. Additionally, for PTF, we confirmed all outburst detections by looking at the individual images. Neither CRTS nor LINEAR images are publicly available at the current time.

We estimate three properties for all outbursting systems presented here: the strength, duration and recurrence time. We define the strength of the outburst to be the difference between the peak luminosity observed and the quiescent magnitude. This is actually a lower limit on the strength, but without continuous monitoring it would be difficult to identify the actual peak magnitude. Our estimates for the properties are consistent with any that exist in the literature.

The outburst duration is even more difficult to determine, due to the infrequent sampling. When available, we used durations from the literature. When not available, we either estimated or placed an upper limit on the duration using our earlier definition of an outburst. For systems with multiple, relatively well-sampled outbursts, we used an average of outburst durations. For systems with only a few observed outbursts and poorly sampled data, we provided an upper limit based on the next detection not in outburst.

The most difficult to estimate is the recurrence time for those systems for which we observed multiple outbursts. Again, we used any published estimates if available, except as noted in Section 3.1. For systems with more than five outbursts, we used the time of the brightest measurement of each outburst, and estimated the recurrence time as their mean. We estimated the error as the scatter of those measurements around the mean, and assumed that the outbursting behaviour remained consistent throughout any gaps in the data. This implies that the recurrence time is fixed, something known not to be true for at least some systems, and thus the error will be a combination of inherent variability in the recurrence time and the exact time of observation at the peak of the outburst. All systems showed a minimum outburst frequency between several outbursts, and we tested longer gaps with integer division to check for any observations at the predicted outburst times. PTF1 J0719+4858 and CP Eri showed extra outbursts that were on time-scales of less than 5 d and outside of the normal pattern of detections. We assumed these to be normal outbursts and ignored them for the purposes of estimating the outburst recurrence time. We generally refrain from using power spectra to estimate recurrence times due to the irregularity and sparsity of measurements relative to the outburst durations, the multiple telescopes, and, oftentimes, the lack of detections in quiescence. Shorter period systems do show some signals corresponding to the observed recurrence times in the power spectra, but these signals are typically weak compared to the noise.

For those systems showing fewer than five outbursts, we estimated the recurrence time as the average time between outbursts. We assigned errors based on a propagation from the uncertainty of duration in the few outbursts observed (i.e. the time from previous observation to observation in outburst), but we emphasize that the few outbursts seen make any error estimation difficult. We tested whether the recurrence time could be our estimate divided by an integral value by looking for observations at the predicted times (a simplistic use of the standard $O - C$ technique). We remark on any adjustments as part of our individual system descriptions in Section 3.1.

3 AM CVN SYSTEMS AND OBSERVATIONAL DATA

We present the known AM CVn systems in Table 1, along with some information on data sources and the presence of outbursts. In this paper, we present only light curves showing significant variability. Combined light curves for all systems, including those which show no variability, are available from the PTF website.[4] Here, we differentiate between three behavioural classes: those systems showing repeated outbursts, those with a single observed outburst, and those with irregular photometric behaviour.

3.1 Regularly outbursting systems

In Figs 1–5 we present outburst light curves of 15 systems with multiple observed outbursts. Two systems known to outburst frequently, PTF1 J1919+4815 and KL Dra, are not presented here due to lack of data in the currently discussed surveys, but we refer the reader to Levitan et al. (2014) and Ramsay et al. (2010), respectively, for detailed analysis of their light curves. We used the outburst criteria detailed in Section 2.2 to identify outbursts in a quantitative fashion, and provide summary data of the outburst characteristics in Table 2. We provide more in-depth discussion on selected systems below. All outburst times are relative to the start of the light curve, which is indicated in the respective figure.

3.1.1 *CR Boo*

CR Boo was found to have a 46.3 d outburst recurrence time by Kato et al. (2000), hereafter K00. However, Kato et al. (2001), hereafter K01, reported that this was not constant and that CR Boo had switched to a 14.7 d recurrence time in 2001. More recent work by Honeycutt et al. (2013), hereafter H13, presents 20 yr of CR Boo photometry and also shows significant changes in its photometric behaviour. The more than 9 yr of regular monitoring presented here

[4] http://ptf.caltech.edu/

Table 1. Known AM CVn systems.

System[a]	Outbursting	Period (min)	Quiescence (g')	PTF[b]	CSS[b]	MLS/SSS[b, c]	LINEAR[b]	References
HM Cnc	N	5.36	20.7	58/59	–	–	–	1
V407 Vul	N	9.48	19.7	–	–	–	–	2
ES Ceti	N	10.3	17.1	–	164/235	–	–	3
KIC 004547333	N	15.9	16.1	117/118	31/36	–	–	4
AM CVn	N	17.1	14.2	103/104	–	–	293/293	5
HP Lib	N	18.4	13.5	–	131/134	S: 130/130	–	6
PTF1 J191905.19+481506.2	Y	22.5	21.5	22/110	–	–	–	7
CR Boo	Y	24.5	17.4	31/31	286/286	–	266/271	8, 9
KL Dra	Y	25.0	19.1	–	–	–	–	10
V803 Cen	Y	26.6	16.9	–	–	S: 231/231	–	6, 11, 12
PTF1 J071912.13+485834.0	Y	26.8	19.4	250/262	281/292	–	–	13
SDSS J092638.71+362402.4	Y	28.3	19.0	8/8	254/295	–	77/714	14, 15
CP Eri	Y	28.7	20.3	198/300	160/228	S: 35/45	–	16
PTF1 J094329.59+102957.6	Y	30.4	20.7	71/217	50/296	M: 51/53	16/1163	17
V406 Hya	Y	33.8	20.5	–	83/262	–	–	18
PTF1 J043517.73+002940.7	Y	34.3	22.3	2/213	7/319	–	–	17
SDSS J173047.59+554518.5	N	35.2	20.1	–	69/119	–	0/535	19, 20
2QZ J142701.6−012310	Y	36.6	20.3	–	62/298	–	19/493	21
SDSS J124058.03−015919.2	Y	37.4	19.7	–	224/302	M: 86/86	39/529	22
SDSS J012940.05+384210.4	Y	37.6	19.8	–	74/260	–	–	14, 23, 24
SDSS J172102.48+273301.2	Y	38.1	20.1	208/298	31/382	–	0/409	25, 26
SDSS J152509.57+360054.5	N	44.3	19.8	80/100	181/254	–	60/231	24, 25
SDSS J080449.49+161624.8	–[d]	44.5	18.2	110/112	336/358	–	–	27
SDSS J141118.31+481257.6	N	46.0	19.4	102/111	84/121	–	0/237	14
GP Com	N	46.5	15.9	11/12	315/315	–	207/450	28
CRTS J045020.8−093113	Y	47.3	20.5	31/66	21/240	–	–	29
SDSS J090221.35+381941.9	Y[e]	48.3	20.2	–	47/341	–	0/337	25, 30
SDSS J120841.96+355025.2	N	52.6	18.8	97/101	283/288	–	101/290	24, 31
SDSS J164228.06+193410.0	N	54.2	20.3	–	1/369	–	0/430	24, 25
SDSS J155252.48+320150.9	N	56.3	20.2	125/242	47/297	–	0/230	32
SDSS J113732.32+405458.3	N	59.6	19.0	72/77	300/309	–	0/539	33
V396 Hya	N	65.1	17.3	54/56	46/48	S: 235/236	–	34
SDSS J150551.58+065948.7	N	–	19.1	143/149	337/347	–	106/606	33
CRTS J084413.6−012807	Y	–	20.3	–	22/324	–	–	35
SDSS J104325.08+563258.1	Y	–	20.3	14/16	22/120	–	34/216	19
PTF1 J221910.09+313523.1	Y	–	20.6	49/72	53/111	–	–	17
CRTS J074419.7+325448	Y	–	21.1	–	103/460	M: 32/49	–	35
PTF1 J085724.27+072946.7	Y	–	21.8	15/126	50/349	–	0/791	17
PTF1 J163239.39+351107.3	Y	–	23.0	61/173	36/324	–	0/564	17
PTF1 J152310.71+184558.2	Y	–	23.5	10/28	2/325	–	0/203	17
SDSS J204739.40+000840.1	Y	–	24.0	–	0/67	–	0/591	31

Note. Systems are sorted by orbital period. System with no orbital period in the literature are at the bottom and sorted by quiescence magnitude.
[a]Names given here are either the IAU variable star name or the full name given in the discovery paper. Throughout this paper, we use a shortened version of the latter.
[b]Survey columns are of the form 'no. of detections/no. of observations'.
[c]Since no system has observations from both MLS and SSS, we use one column for both surveys and indicate the appropriate survey.
[d]SDSS J0804+1616 has non-outburst variability. See Section 3.3.
[e]SDSS J0902+3819 was recently reported to outburst (Kato et al. 2014). Our data here do not include this outburst.
References: (1) Roelofs et al. (2010); (2) Steeghs et al. (2006); (3) Espaillat et al. (2005); (4) Fontaine et al. (2011); (5) Roelofs et al. (2006b); (6) Roelofs et al. (2007a); (7) Levitan et al. (2014); (8) Patterson et al. (1997); (9) Kato et al. (2000); (10) Ramsay et al. (2010); (11) Patterson et al. (2000); (12) Kato et al. (2004); (13) L11; (14) Anderson et al. (2005); (15) Copperwheat et al. (2011); (16) Groot et al. (2001); (17) Levitan et al. (2013); (18) Roelofs et al. (2006a); (19) Carter et al. (2013); (20) Carter et al. (2014a); (21) Woudt, Warner & Rykoff (2005); (22) Roelofs et al. (2005); (23) Shears et al. (2011); (24) Kupfer et al. (2013); (25) Rau et al. (2010); (26) Augusteijn private communication; (27) Roelofs et al. (2009); (28) Nather, Robinson & Stover (1981); (29) Woudt et al. (2013); (30) Kato et al. (2014); (31) Anderson et al. (2008); (32) Roelofs et al. (2007c); (33) Carter et al. (2014b); (34) Ruiz et al. (2001); and (35) Breedt et al. (2014).

provides a complementary view of CR Boo's behaviour, particularly in the time period since 2004 when H13's sampling is much more irregular.

The most surprising feature of the long-term light curve presented is a clear distinction in behaviour between the first ∼4.5 yr and the remaining data (Fig. 1). We will refer to these separate parts of the light curve as the 'active' and 'inactive' states. In the active state (2452647 < HJD < 2454337), CR Boo was only observed between $14 < V < 16$. In contrast, during the inactive state (2454337 < HJD < 2456147), CR Boo was observed near its quiescent state ($V < 16$) ∼50 per cent of the time. The abrupt change in behaviour is present in both the LINEAR and CSS data.

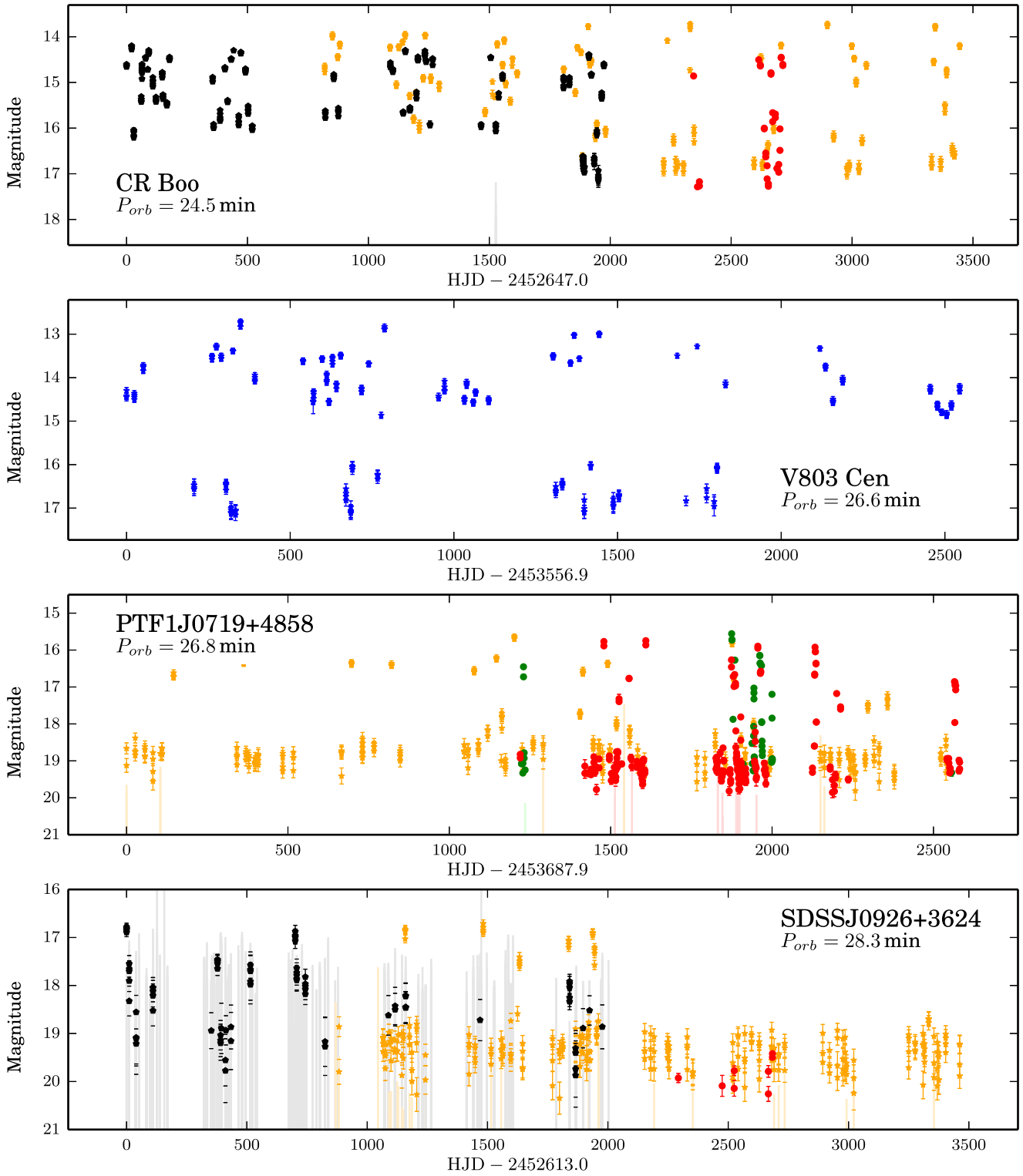

Figure 1. Light curves of the four shortest period regularly outbursting AM CVn systems presented here. All show regular changes from quiescence to outburst (Section 3.1). In particular, we point out the significant change in the behaviour of CR Boo (Section 3.1.1) and of SDSS J0926+3624 (Section 3.1.3). Legend: black = LINEAR; yellow = CSS; blue = SSS; red = PTF R; and green = PTF g'. The tops of the vertical lines (colour-coded to match the survey) are limiting magnitudes for non-detections.

Although an obvious step is to search for periodicity in the data, the infrequent and uneven sampling of the CSS and LINEAR surveys prevents a comprehensive analysis. Without compelling evidence, even a peak with significant power in a periodogram may be false. Instead, we consider the recurrence time during CR Boo's inactive state by using a set of observations from the P60 that were taken over ∼160 d and with a nominal cadence of 3 d. This provides a much better data set for period analysis. The peak of the

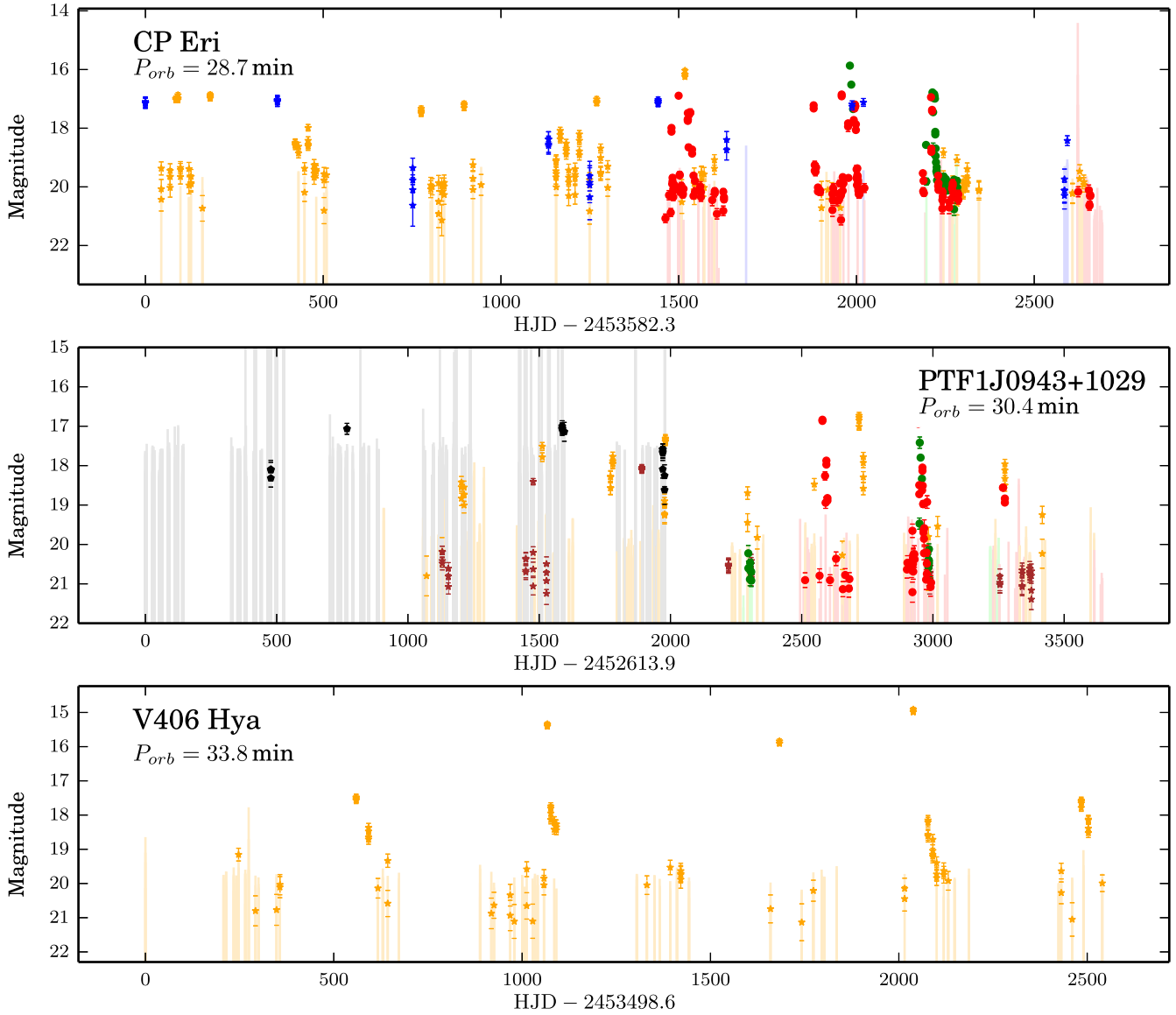

Figure 2. Light curves of three regularly outbursting AM CVn systems in order of $P_{\rm orb}$, which all show regular changes from quiescence to outburst (Section 3.1). In contrast with the light curves in Fig. 1, all systems in this figure spend the majority of their time in quiescence with only occasional outbursts. This is particularly true for V406 Hya. Legend: black = LINEAR; yellow = CSS; blue = SSS; maroon = MLS; red = PTF R; and green = PTF g'. The tops of the vertical lines (colour-coded to match the survey) are limiting magnitudes for non-detections.

periodogram for the P60 observations is at 46.5 d. This estimate is consistent with the outburst recurrence time found by K00. We present these observations, a periodogram generated from them, and a folded light curve in Fig. 6.

We estimate an error of 10.5 d for this period by a bootstrap process (Efron 1982). To calculate the error, we drew, at random, 68 observations from the total set of 68 observations, allowing for repetition. This randomizes both the number of observations and which observations are used. We then calculated a Lomb–Scargle periodogram (Scargle 1982) for the randomly drawn data, and recorded the peak. We repeated this process 500 times, and used the standard deviation as the error estimate.

We now use the much more extensive data for CR Boo from the LINEAR and the CSS surveys, and again compute a periodogram. Here we have a peak at 47.6 d ± 4.8 d. We present a periodogram and folded light curve in Fig. 7.

The outburst recurrence time is statistically consistent between the P60 observations, the LINEAR and CSS observations, and the earlier work by K00 and H13. In particular, H13 found a dominant spacing between outbursts of 46 d over 20 yr. It is thus likely that the dominant outburst recurrence time is the same between active and inactive states and is around 46 d. For the analysis in this paper, we use the value we derived from the LINEAR and CRTS data, as it is derived from 5 yr of data.

Our data are in agreement with those of H13, specifically regarding the changing state of CR Boo. However, H13 show even more variability in the long-term light curve, particularly during the time period that is not covered by the data presented here (1990–2000). We believe that CR Boo's inactive state between 2005 and 2010 has been remarkably stable, particularly given the relatively clean outburst light curves presented here. It is obvious that the system often experiences rapid changes in its behaviour.

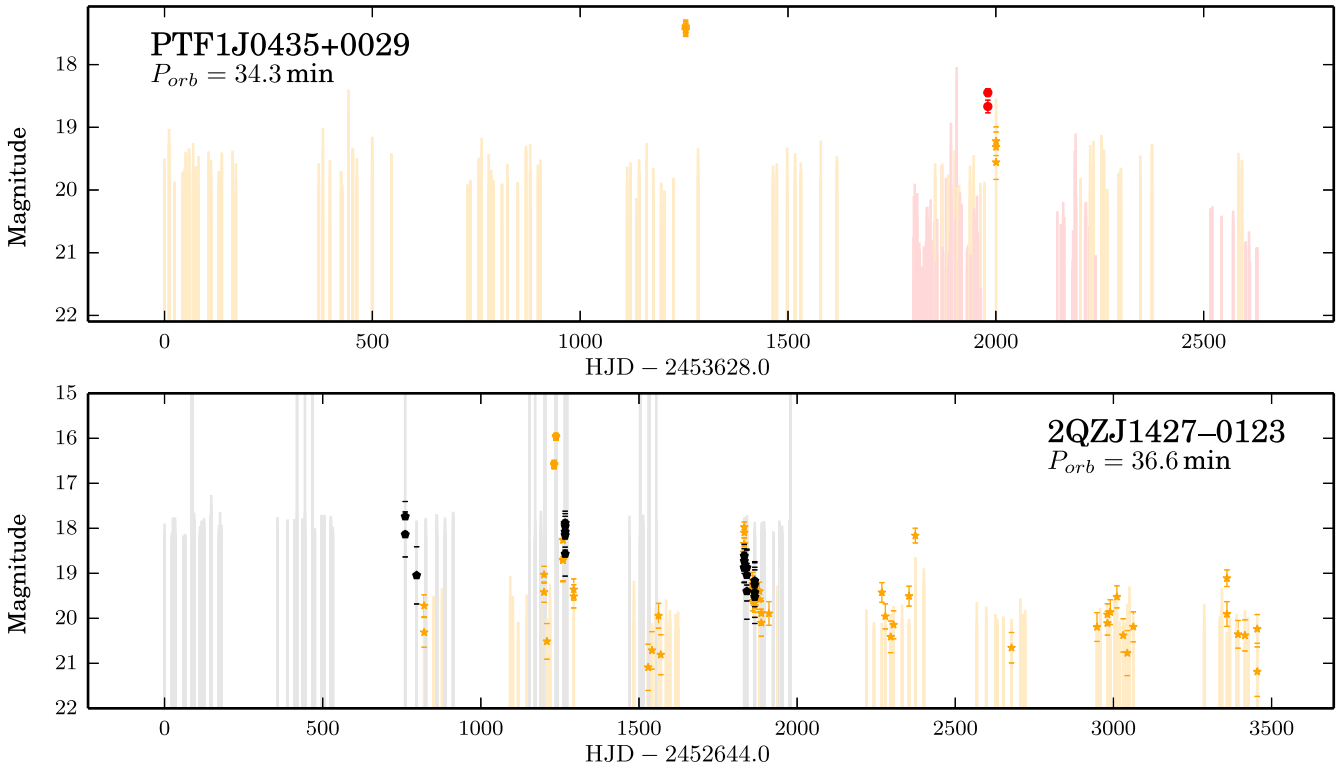

Figure 3. Light curves of the two longest period, known, regularly outbursting AM CVn systems. Both systems show only a few outbursts with recurrence times of ≥1 yr. Legend: black = LINEAR; yellow = CSS; and red = PTF *R*. The tops of the vertical lines (colour-coded to match the survey) are limiting magnitudes for non-detections.

3.1.2 V803 Cen

V803 Cen was found by Kato et al. (2004) to have a 77 d outburst recurrence time with very similar characteristics to the active state of CR Boo described in Section 3.1.1. In contrast to CR Boo, the light curve presented here (Fig. 1) shows no significant changes in the amplitude of photometric variability over almost 7 yr. We see no coherent light curve when folded at the recurrence time given by Kato et al. (2004). No significant period in a periodogram calculated from the SSS data results in a coherent light curve either, which is consistent with the data of CR Boo in its active state. We thus use the period found by Kato et al. (2004) for our analysis in this paper and assume a 10 per cent error, consistent with the variability in the outburst recurrence times of CR Boo, KL Dra, and PTF1 J0719+4858 (see Table 1 for references). It is possible that this lack of periodicity is due to changing outburst recurrence times, as seen for CR Boo during its active state (Section 3.1.1).

3.1.3 SDSS J0926+3624

SDSS J0926+3624 is perhaps the best understood AM CVn system, given its deep eclipses. Copperwheat et al. (2011) reported on two outbursts and showed the CSS light curve. The light curve we present here has both additional historical data from the LINEAR survey, as well as newer data from the CSS. Similarly to CR Boo, SDSS J0926+3624 shows a dramatic change in behaviour roughly half-way through the light curve (Fig. 1). The earlier part of the light curve (HJD $\lesssim$ 2461620) shows repeated outbursts, with a recurrence time of 140–180 d.

The latter part of the light curve (HJD $\gtrsim$ 2461620), however, does not show any outbursts. Given that the cadence of CSS did not change, this is surprising, and is likely an indicator of a real change in the system. We do know that at least one outburst was missed in the CSS coverage – that reported in Copperwheat et al. (2011) to have occurred in 2009 March. Although it is possible that others were missed as well, we estimate only a ∼4 per cent probability of a missed outburst, based on times between CSS observations, the expectation of an outburst at least every 180 d with a duration of at least 20 d, and not accounting for any particular pattern of outburst relative to the previous outburst. This implies that the outburst behaviour of SDSS J0926+3624 likely changed, whether to less frequent outbursts or ones that return to quiescence faster.

3.1.4 CP Eri

Previous studies of AM CVn systems have identified only a few outbursting systems that show both superoutbursts and normal outbursts. These systems (PTF1 J1919+4815, CR Boo, and PTF1 J0719+4858) have some of the shortest known orbital periods of the outbursting systems. The normal outbursts are typically 1–2 d in length and appear to have a similar or slightly lower strength as superoutbursts (e.g. K00, L11). The data presented here show that CP Eri (Fig. 2), a slightly longer period system with $P_{\rm orb} = 28.7$ min, also appears to show normal outbursts. Three increases in brightness of at least two magnitudes between superoutbursts are constrained to last fewer than five days – consistent with what would be expected for a normal outburst. This likely indicates that other longer period AM CVn systems also show normal outbursts in addition to superoutbursts.

3.1.5 PTF1 J0435+0029

In 7 yr of coverage with the CSS and the PTF, PTF1 J0435+0029 was observed in outburst twice (Fig. 3). Given the faint nature

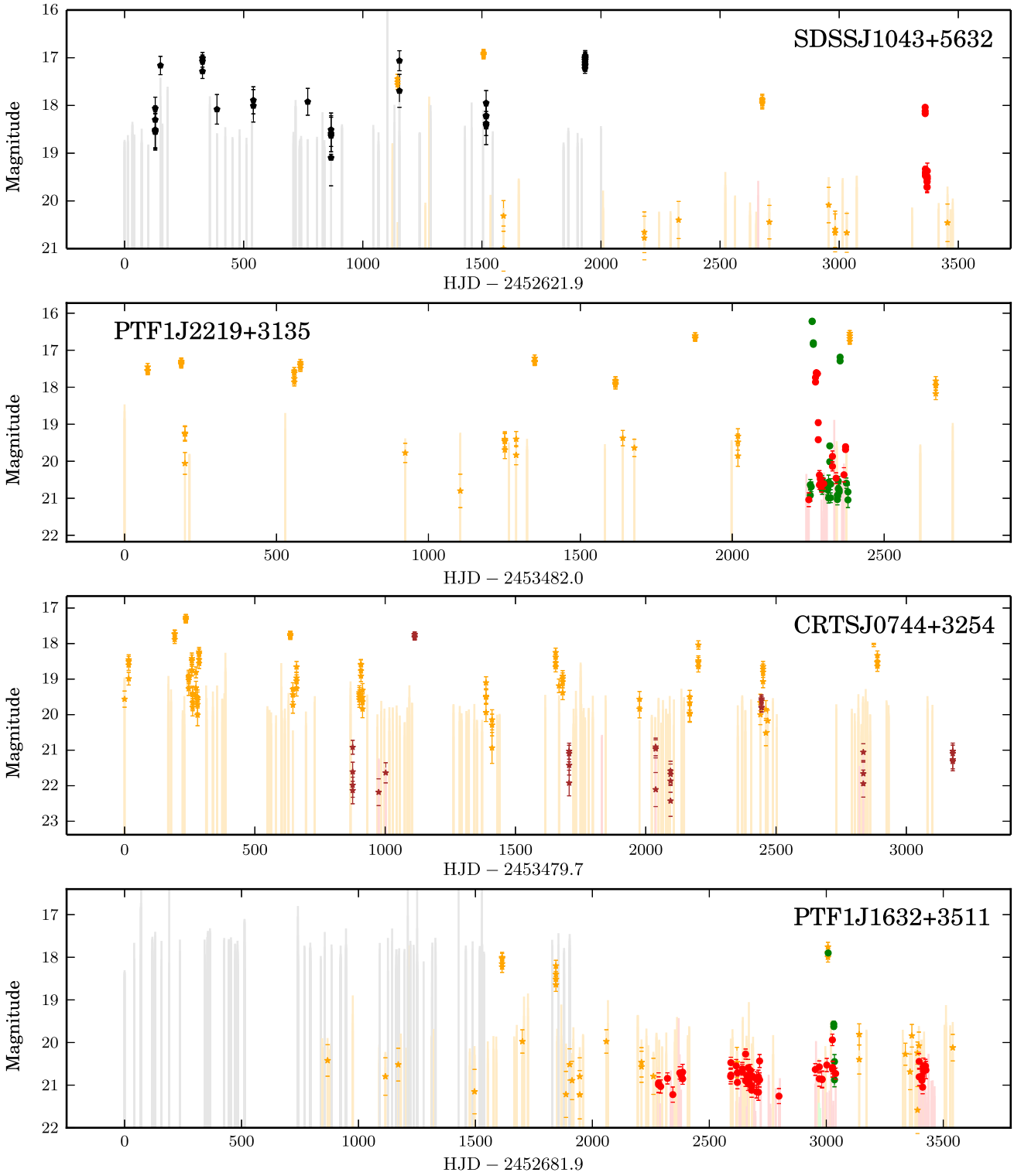

Figure 4. Light curves of four regularly outbursting AM CVn systems with unknown orbital periods. We use their outburst recurrence times to estimate orbital periods in Section 4.2.2. Legend: black = LINEAR; yellow = CSS; red = PTF R; and green = PTF g'. The tops of the vertical lines (colour-coded to match the survey) are limiting magnitudes for non-detections.

of the system, only an observation at the very beginning of the outburst would be above the limiting magnitude of both surveys, and thus the lack of additional outbursts is not surprising. The two observed outbursts were ∼730 d apart ($t = 1250 \pm 30$ d and 1980^{+50}_{-8} d), but the time half-way between had no observations, and hence both 365 and 730 d recurrence times are consistent with the data. Here, we use the former, as the latter would be a significant outlier from the remainder of the AM CVn systems (see Table 2). Only further observations can remove this ambiguity.

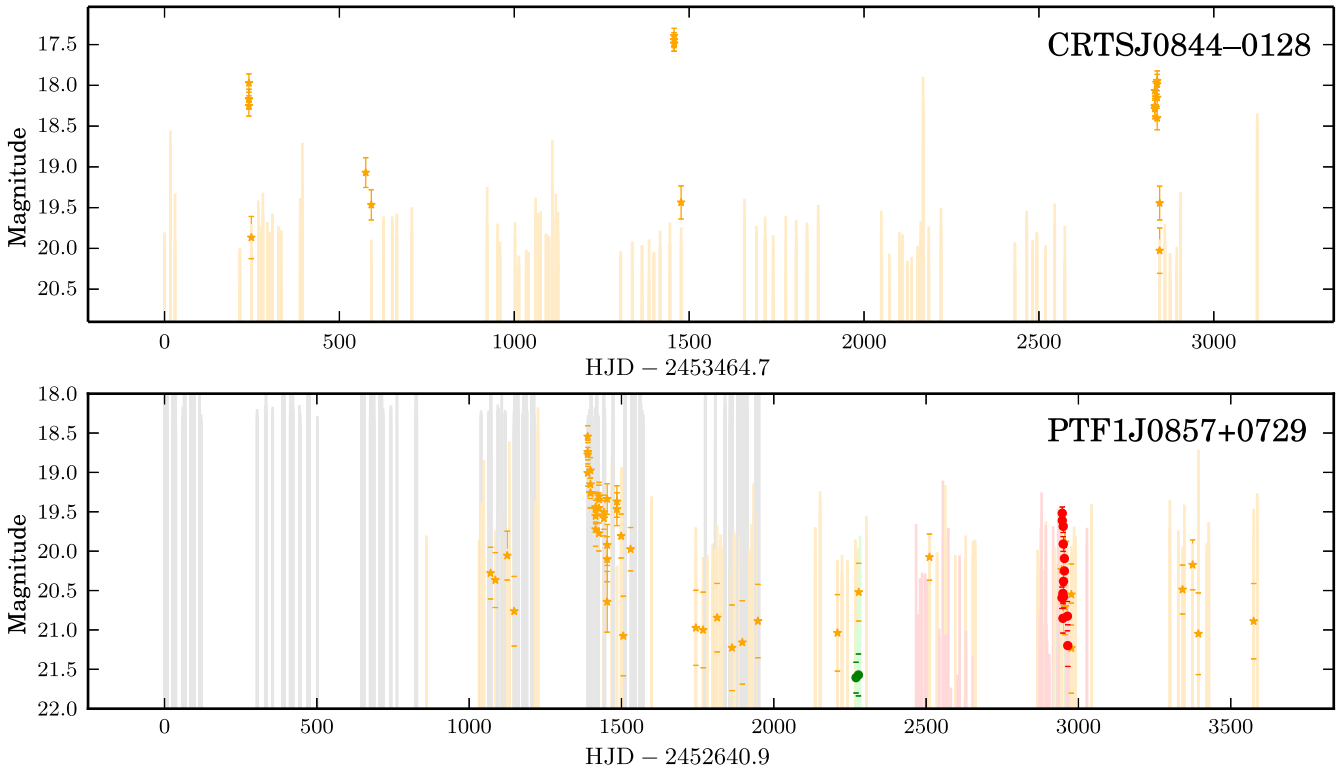

Figure 5. Light curves of two regularly outbursting AM CVn systems with unknown orbital periods and extremely long outburst recurrence times. These are discussed in Section 3.1.7. Legend: black = LINEAR; yellow = CSS; red = PTF R; and green = PTF g'. The tops of the vertical lines (colour-coded to match the survey) are limiting magnitudes for non-detections.

Table 2. Outburst properties of recurring outburst systems with known orbital periods.

System	orbital per. (min)	No. of outbursts pbserved	Observation span (d)	Recurrence time (d)	Duration (d)	Strength (mag)
PTF1 J1919+4815[a]	22.5	–	–	36.8 ± 0.4	∼13	3
CR Boo[b]	24.5	–[c]	3445	47.6 ± 4.8	∼24	3.3
KL Dra[a]	25.0	–	–	44–65	∼15	4.2
V803 Cen[a]	26.6	–[c]	2545	77	–	4.6
PTF1 J0719+4858[a]	26.8	23	2581	65–80	∼18	3.5
SDSS J0926+3624	28.3	9	3462	160 ± 20	∼20	2.4
CP Eri	28.7	13	2691	108 ± 13	∼20	4.2
PTF1 J0943+1029	30.4	10	3645	110 ± 14	<30	4.1
V406 Hya	33.8	5	2540	280 ± 50	<100	5.9
PTF1 J0435+0029	34.3	2	2629	365 ± 60	<60	5.1
2QZ J1427−0123	36.6	3	3455	540 ± 60	<50	4.3

Note. Definitions of the properties shown here are in Section 2.2.
[a]Properties presented here (except observation details) are from the literature. See Table 1 for references.
[b]The reported data are from only the second half of CR Boo observations presented in this paper (see Section 3.1.1).
[c]We do not count the number of outbursts due to the complicated and rapidly changing nature of the light curve.

3.1.6 2QZ J1427−01

We find three outbursts for 2QZ J1427−01 (Fig. 3), with peak magnitudes at $t = 760^{+40}_{-50}$, 1240^{+30}_{-20}, and 1830^{+10}_{-30} d. We constrain the duration of the outbursts to <50 d, based on the second outburst. We provide estimates for the remaining two outbursts using this outburst duration to obtain a lower bound on their times of peak luminosity, since both outbursts occurred before the start of an observing season. The mean difference between these peaks is 540 ± 65 d, with the error derived based on the errors of each outburst peak. We note that this is roughly consistent with the 10–20 per cent change in outburst recurrence time observed in shorter period systems.

These outbursts occur over a period of ∼1000 d, while we have data over a time span of >3500 d. We thus expect additional outbursts at $t \approx 210$, 2370, 2910, and 3450 d. The first falls between observing seasons, while the third and fourth are just before and after an observing season, respectively. Given the associated error, it is highly likely that no outburst would have been seen. There are observations at $t = 2354$, 2374, and 2401 d, roughly coincident with when we would expect an outburst. One of the exposures on

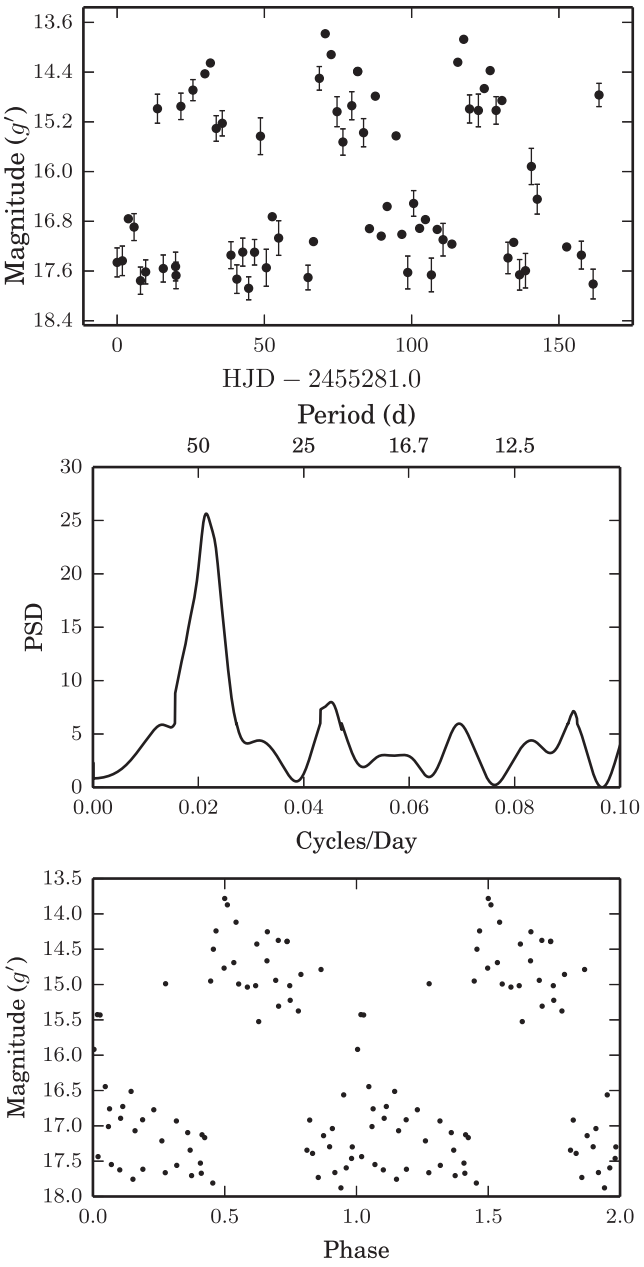

Figure 6. Top: the un-folded light curve of CR Boo taken by the P60. Three outbursts are clearly visible. We use this much higher cadence and more regular light curve to establish that a period of ∼50 d is real. Middle: a periodogram of the CR Boo P60 data, showing a peak at 46.5 d. Bottom: the CR Boo P60 data light curve folded at the peak period of 46.5 d, with the peak of the outburst set to a phase of 0.5. The outburst and quiescent portions of the light curve are clearly separated.

$t = 2374$ d does show a detection consistent with an outburst, while the remaining three exposures do not indicate outbursts. This may indicate that the system was at the end of an outburst. We note that the data obtained by R12 do not provide coverage of these predicted outburst times.

We also consider whether the outburst recurrence time may be shorter. A recurrence time of one-half the proposed value would require outbursts at $t = 1560$ and 2640 d, both of which are in the middle of observing seasons. Likewise, one-third of the proposed value also shows coverage during times of expected outbursts. We

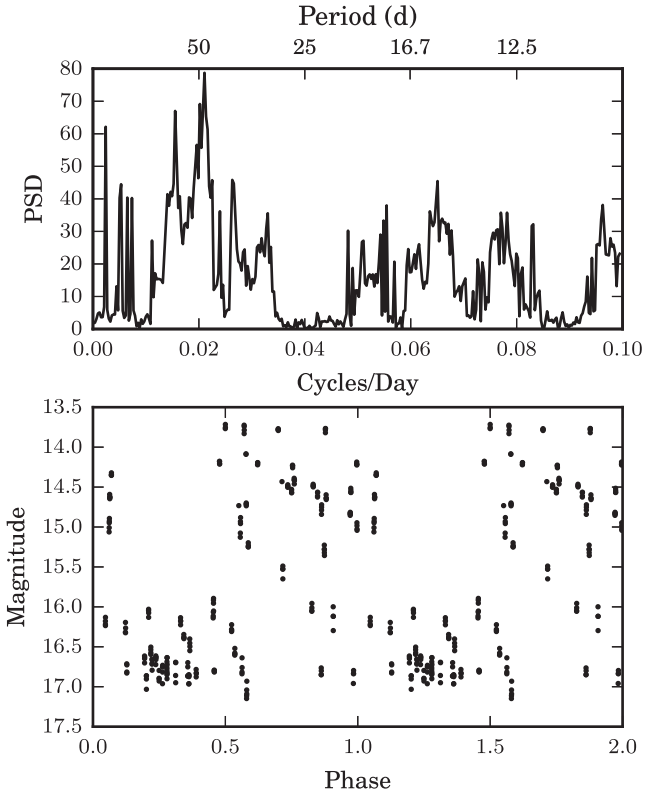

Figure 7. Top: a periodogram of the CSS and LINEAR data of CR Boo. The strongest peak is at 47.6 d, with an associated error of 4.8 d. Only with the proof from the P60 data in Fig. 6 do we believe that this is a real period. Bottom: a folded light curve of the CSS and LINEAR data of CR Boo's while it is in its inactive state. The data are folded at the above period of 47.6 d, and show a clear outburst and quiescent states. The recurrence time is consistent over 5 yr.

thus conclude that 2QZ J1427−01 has an outburst recurrence time of 540 ± 65 d.

3.1.7 CRTS J0804−0128 and PTF1 J0857+0729

Two systems, CRTS J0804−0128 and PTF1 J0857+0729, have only a few recorded outbursts but with other observations almost at the level of an outburst. The outburst recurrence time for the former is approximately 1300 d while for the latter it is approximately 1550 d. Such recurrence times are not similar to the other systems presented here. Given the lack of measured orbital periods for either system, we do not know if these long outburst recurrence times indicate much longer period systems or if their outbursts were simply not observed. We thus refrain from further analysis of these systems.

3.2 'Single outburst' systems

Seven of the known AM CVn systems have only had a single outburst recorded. We present the light curves of these systems in Figs 8 and 9. Drawing on our observations, as well as those reported in the literature, we list outburst times and strengths, as well as the probability of a missed outburst, in Table 3. We present the outburst light curves for four of the systems with the most details in Fig. 10.

We focus on the data here, and leave out discussion of these systems and whether they are truly one-time outbursts until our

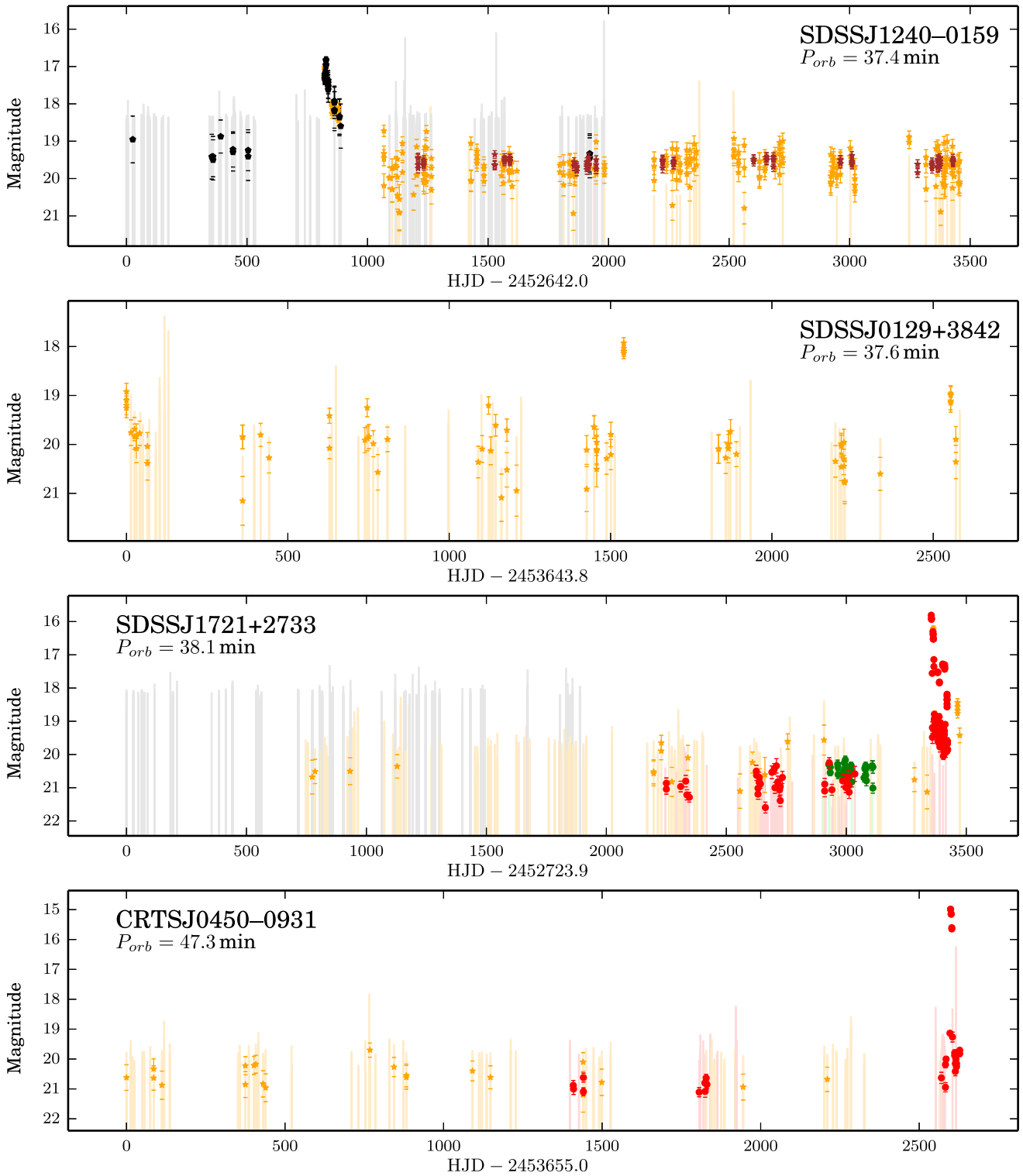

Figure 8. Light curves of the four outbursting AM CVn systems with only one recorded outburst. All systems have longer orbital periods than the regularly outbursting AM CVn systems. In the case of SDSS J0129+3842, two additional possible outbursts are visible, but they do not meet our criteria for an outburst (Section 2.2). Legend: black = LINEAR; yellow = CSS; maroon = MLS; red = PTF R; and green = PTF g'. The tops of the vertical lines (colour-coded to match the survey) are limiting magnitudes for non-detections.

discussion in Section 4.2.3. The most important question to answer is to calculate the probability of a missed outburst. We use a Monte Carlo approach where, for each of 1000 iterations for each system, we tested whether an outburst starting at a random time between the start and end points of the light curve would be detected. A system in outburst was assumed to be detected if it was 1.5 mag above quiescence and greater than the limiting magnitude for that exposure. We required at least two detections over the course of

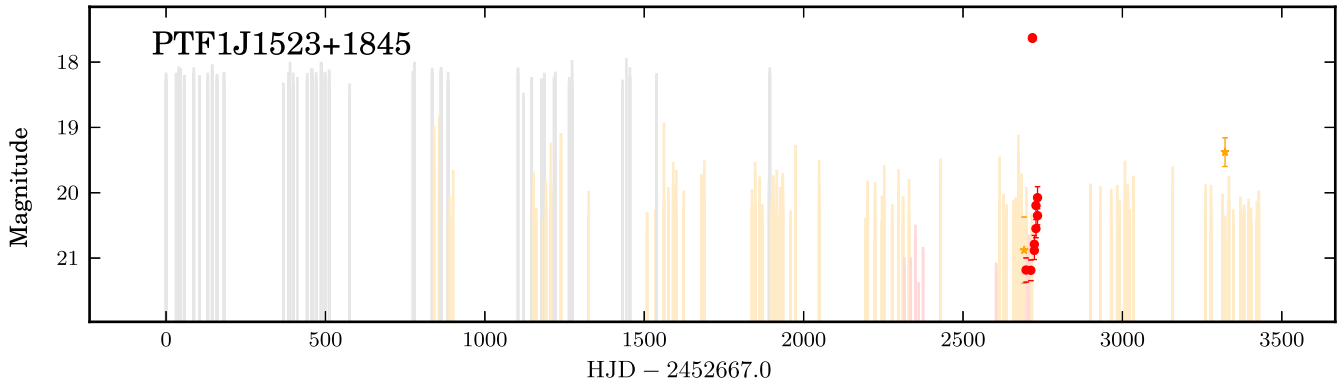

Figure 9. Light curve of PTF1 J1523+1845, a single outburst AM CVn system with no known orbital period. Legend: black = LINEAR; yellow = CSS; and red = PTF *R*. The tops of the vertical lines (colour-coded to match the survey) are limiting magnitudes for non-detections.

Table 3. Details of single outbursts.

System	Outburst date	Strength[a] (mag)	Probability of missed outburst
SDSS J0129+3842	2009 Nov. 29	∼5.4	0.78 ± 0.02
CRTS J0450−0931	2012 Nov. 22	∼5	0.75 ± 0.02
SDSS J1240−0159	2005 March 15	∼6	0.18 ± 0.01
PTF1 J1523+1845	2010 July 07	∼5.8	0.78 ± 0.02
SDSS J1721+2733	2012 May 30	∼5	0.59 ± 0.02
SDSS J2047+0008	2006 Oct. 12	∼5	1.0

Notes. The data presented in this table are drawn from a combination of the referenced papers and the light curves presented here. Systems are arbitrarily ordered in terms of RA.
[a]The numbers presented here are lower bounds since the outburst peak was not always caught.

the outburst. This itself was repeated 100 times, and the standard deviation of these 100 runs is the reported error for the probability of non-detection. The detection threshold was set in agreement with our definition of an outburst in Section 2.2 and the scatter of points in quiescence for all these systems was ∼0.5 mag.

For this to work effectively, we must use a reasonable model of the light curve. We note that for all but SDSS J1240−0159, the post-peak outburst light curve consists of a sharp decline that reaches 1–2 mag above quiescence within 10 d, and then a gradual decline over 30–60 d. We base this not only on our data (Fig. 10) but on similar light curves for SDSS J0129+3842 in fig. 4 of R12 and SDS J2047+0008 in fig. 4 of Anderson et al. (2008). We model all three systems by using an inverse parabola that reaches 1.5 mag above quiescence after 10 d, and then a linear decline over the next 50 d back to quiescence. The only difference in our model between the systems is the initial outburst peak magnitude. In the case of SDSS J1240−0159, we assume a simple linear decline from peak to quiescence over 80 d. This difference accounts for the significantly different shape of the outburst (Fig. 10). The results of these calculations are listed in Table 3.

We make three observations here based on these results. First, it is not surprising that SDSS J2047+0008 was not detected in our data, given its short outburst duration and quiescent magnitude of $g' \sim 24$ (Anderson et al. 2008). Secondly, out of the rest of the systems, only SDSS J1240−0159 is likely to have not had a missed outburst. Its outburst shape, as noted earlier, is very different than the other systems. Finally, SDSS J1721+2733 shows re-brightening events during its decline (see Fig. 10), something also reported for SDSS J0129+3842 (Shears et al. 2011).

3.3 Other variability

R12 noticed that SDSS J0804+1616 showed significant variability, but not of the typical outburst variety. Instead, it showed irregular variability with an amplitude of ∼1 mag. The light curve we present in Fig. 11 confirms this variability over 7 yr. We find no discernible period, although the time-scale of the variability could be as short as 1–2 nights, based on several nights where the target was observed ∼15 times in one night by the PTF. Roelofs et al. (2009) suggested that SDSS J0804+1616 may be a magnetic system. Similar light curves have been observed in PTF for magnetic CVs (Margon et al. 2014), strengthening the argument that SDSS J0804+1616 is, in fact, a magnetic system.

We also present the light curve of SDSS J1730+5545 in Fig. 11. The light curve contains what appears to be the tail end of an outburst. However, despite multiple detections at ∼1.5 mag brighter than the median magnitude, it fails to meet our criteria for the definition of an outburst. Similarly, SDSS J0129+3842 also shows at least two other candidate outbursts, both of which fail to meet our criteria. We are reluctant to loosen the criteria, however, as SDSS J1730+5545 is the only system where just a partial outburst may have been detected. We note that SDSS J1730+5545's recently measured orbital period of 35.2 min (Carter et al. 2014a) places it at the long end of the outbursting orbital period regime, but poor coverage makes the concrete detection of an outburst difficult given outburst recurrence times of systems with similar orbital periods.

4 RESULTS AND DISCUSSION

4.1 AM CVn system evolution

The composite light curves presented here allow us to see long-term changes in the photometric behaviour of AM CVn systems. We summarize the phenomenology of outbursting AM CVn systems in the following three stages of evolution.

(i) When the mass transfer rate from the secondary ($\dot{M}$) falls below a critical value (believed to occur for $P_{\rm orb} \gtrsim 20$ min), the accretion disc is no longer in a high state at all times and instabilities in the disc develop that lead to large amplitude photometric variations. The light curves of the shortest period systems in this study (CR Boo and V803 Cen) show that the transition from a stable high state to 'regular' outbursts is in fact irregular with variations on long time-scales (years). The systems can spend most of their time in a high state with occasional excursions to the quiescent state (as has been observed exclusively for V803 Cen) or act as a

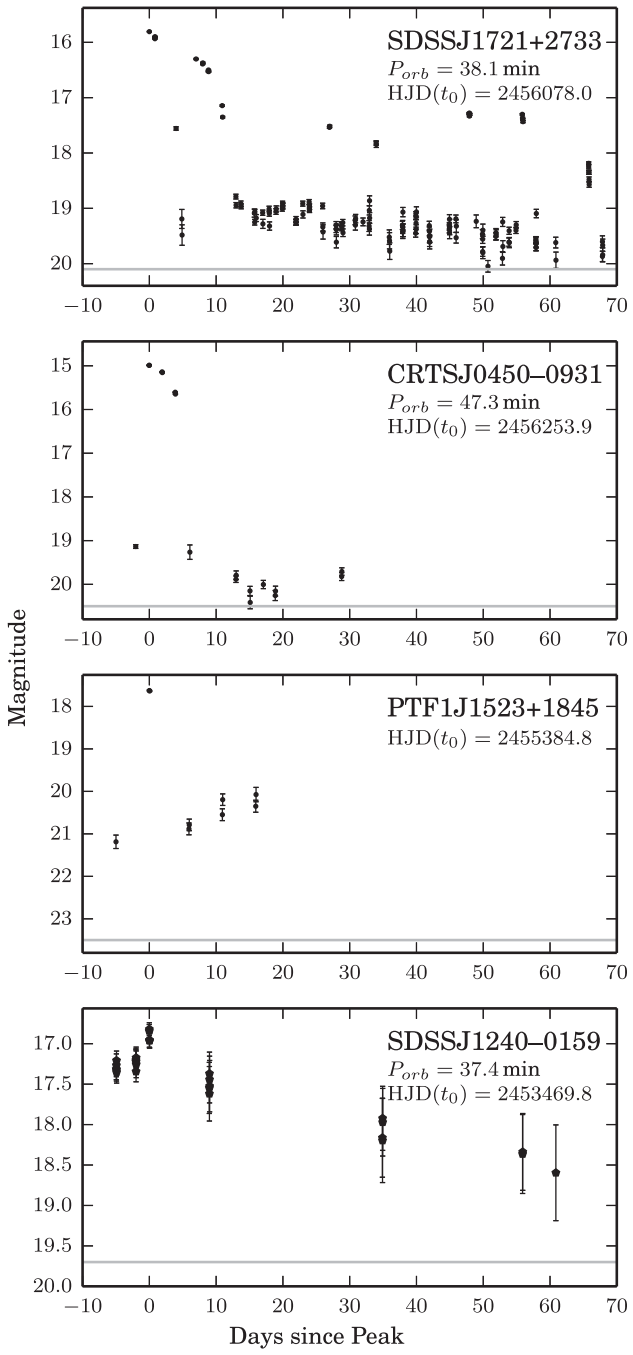

Figure 10. A plot of the outburst light curves for four of the single outburst systems. SDSS J1240−0159 is from LINEAR data and the rest are PTF *R*-band data. The grey line indicates the quiescence level of each system. We note the similarity between the light curves of SDSS J1721+2733 and CRTS J0450−0931, and, to a lesser extent, likely due to lack of data, PTF1 J1523+1845. All three systems show a sharp rise, a fall within 10 d, and a gradual decline towards quiescence. On the other hand, the light curve of SDSS J1240−0159 shows a gradual decline from peak and is still >1.5 mag brighter than quiescence 60 d from the peak of the outburst.

more 'traditional' outbursting system – remaining primarily in the quiescent state, with semiregular outbursts to the high state.

(ii) Only for $P_{\rm orb} \gtrsim 28$ min do systems seem to settle into a more regular pattern of quiescence with well-defined outbursts. Between orbital periods of roughly 28 and 37 min, AM CVn systems are primarily quiescent with somewhat regular outbursts, the properties of which exhibit a gradual process of a power law increase in recurrence time (see Section 4.2 for details). Normal outbursts still occur, but are rarer and longer than in shorter period systems.

(iii) At longer orbital periods, $\dot{M}$ has decreased significantly and systems experience rare outbursts, if any. These systems may be the analogues to WZ Sge systems among the CVs, but the short outburst durations (∼10–15 d) of all known systems except SDSS J1240−0159 do not fit with this analogy. One possible explanation is that such short outbursts are the equivalent of the normal outbursts seen in much shorter period systems (e.g. Section 3.1.4). The outburst of SDSS J1240−0159, which shows a significantly longer duration than the remaining systems, would then be a superoutburst. Its outburst properties are, in fact, consistent with the relations we find in Section 4.2. If this proposal is correct, then the recurrence time of these shorter duration outbursts could be on the order of years, while the recurrence time of superoutbursts could be decades. Such a recurrence time would be consistent with those seen in WZ Sge systems, but no normal outbursts have been observed in WZ Sge systems (Matthews et al. 2007). However, the significantly different composition of the systems (He-rich versus H-rich) and the resulting significant difference in both separation between the components and component temperatures may account for this difference in behaviour. Additional study of the recently discovered He-rich CVs with orbital periods similar to those of the longest known AM CVn systems (Breedt et al. 2012) may help resolve this question.

It is obvious that orbital period is not the only factor influencing the behaviour of these systems, and other factors, likely the component masses, donor composition, and donor entropy will play a role. For example, V406 Hya has significantly stronger outbursts than other systems of comparable orbital periods (see Table 2). Additionally, transitions between states may result in unstable photometric behaviour: CR Boo and SDSS J0926+3624 are possible examples of such systems.

4.2 Outburst behaviour versus orbital period

The change in outburst behaviour with orbital period appears to be gradual, rather than abrupt. While there are only data for a limited number of systems, these are enough to find an approximate relation. For the outburst recurrence time and duration we chose to use a power-law model, while for the strength, Δmag, we used a linear model in magnitudes (this corresponds to an exponential model in flux). These choices are somewhat arbitrary and are only a simple phenomenological approximation to any physical relation. An exponential model fits the outburst recurrence time and duration equally well (see Appendix A) but a power law is consistent with the orbital evolution equations proposed for AM CVn systems (Faulkner et al. 1972). Using the values from Table 2, we find the following relations:

$$P_{\rm recur} = (1.53 \times 10^{-9}) P_{\rm orb}^{7.35} + 24.7$$

$$\Delta{\rm mag} = 0.13 P_{\rm orb} - 0.16$$

$$t_{\rm dur} = (2.53 \times 10^{-6}) P_{\rm orb}^{4.54} + 10.6,$$

where $P_{\rm orb}$ is the orbital period in minutes, $P_{\rm recur}$ is the outburst recurrence time in days, Δmag is the strength of the outburst, and $t_{\rm dur}$ is the duration of the outburst in days. A plot of these quantities, together with the best fits, are shown in Fig. 12. We provide complete

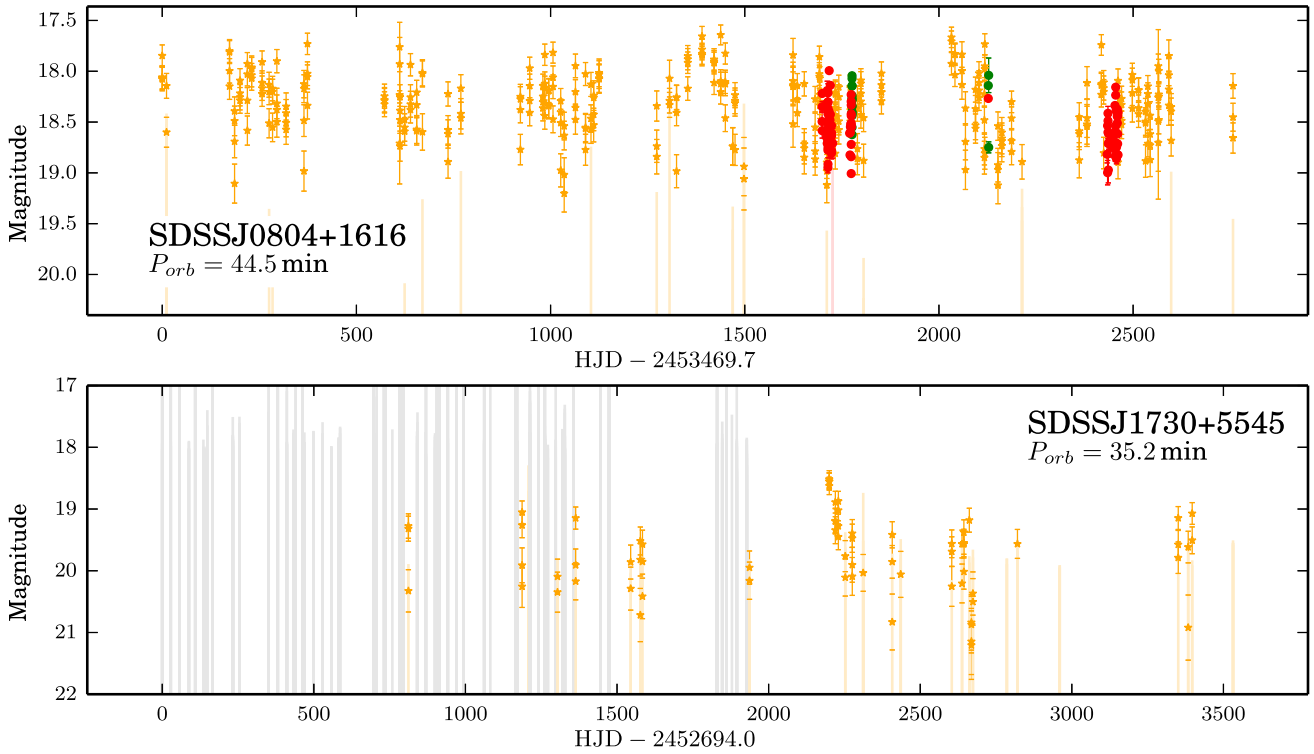

Figure 11. Light curves of two systems with non-outburst variability (Section 3.3). SDSS J0804+1616 is possibly a magnetic system (Roelofs et al. 2009) and shows non-periodic variability akin to that seen in magnetic CVs. SDSS J1730+5545 shows a potential outburst, but one which does not meet our criteria. Legend: black = LINEAR; yellow = CSS; red = PTF R; and green = PTF g'. The tops of the vertical lines (colour-coded to match the survey) are limiting magnitudes for non-detections.

fit details, including information about the fit errors, in Appendix A. The outburst recurrence time is a much better fit than the duration or strength – this may be due to either measurement errors or because AM CVn systems vary more in outburst strength and duration than in recurrence time. We also do not account for the progenitor type of each system (e.g. Nelemans et al. 2010), although it is possible that this has an impact on system outburst behaviour.

Verification of these relations will require significant additional period measurements. We note that these relations do not apply to systems with only one observed outburst, and we do not recommend applying them to systems with only a few observed outbursts. It is highly likely that, particularly at the long-period end, these relations are not accurate due to the lack of data in that period regime. In particular, the single outburst systems identified in this paper typically show an outburst duration of only 10–15 d (see Fig. 10), whereas t_{dur} trends towards 50 d at a similar orbital period.

We also note that these relations apply only to optical wavelengths. AM CVn systems have been poorly studied in other wavelengths, although the few systems observed have been seen to vary in other wavelengths. In particular, KL Dra was observed in UV and X-ray by Ramsay et al. (2010) and SDSS 1043+5632 shows variability of 3.7 mag over 26 NUV observations in the Second *GALEX* Ultraviolet Variability Catalog (Wheatley, Welsh & Browne 2008). Future UV missions (e.g. ULTRASAT; Sagiv et al. 2014) will help better explain UV variability in AM CVn systems.

4.2.1 Are the outburst property relationships realistic?

Our fits make two substantial assumptions: first, that all three properties we model (outburst recurrence time, duration, and strength) are increasing with respect to P_{orb} and, secondly, that the relationships are dependent only on P_{orb}. We aim to verify whether both of these are true.

To ascertain the correlation between P_{orb} and the outburst properties, we calculate the Spearman rank correlation coefficient for 100 000 unique, random permutations of the property values. The fraction of the permutations for which the coefficient is greater than for the data points in order (indicating that this set of points is more correlated with P_{orb} than the original set) is the p-value that the property is not correlated with the orbital period (with a p-value of 0 indicating high probability of correlation and 1 indicating a low probability of correlation). We find that the p-values for recurrence time, outburst strength, and duration are, respectively, 0.00, 0.026, and 0.0057. These indicate that the recurrence time and, to a slightly lesser extent, the duration, are strongly correlated with P_{orb}, while outburst strength is slightly less correlated.

We thus conclude that it is very likely that all the properties are correlated with P_{orb}. However, are they only dependent on P_{orb} or do other system properties influence this as well? If, in fact, the relationships are dependent only on P_{orb} and the correct model is being used, then the residuals should be distributed around zero with a normal distribution. We use the Shapiro–Wilk test (Shapiro & Wilk 1965) to calculate the probability that the residuals are taken from a normal distribution (although we find that related tests provide similar results). The p-values for the recurrence time, outburst strength, and outburst duration are, respectively, 0.03, 0.81, and 1.1×10^{-4}; these represent the probability of observing such residuals had they been normally distributed.

While the outburst strength is normally distributed, both the recurrence time and outburst duration are likely not. This indicates

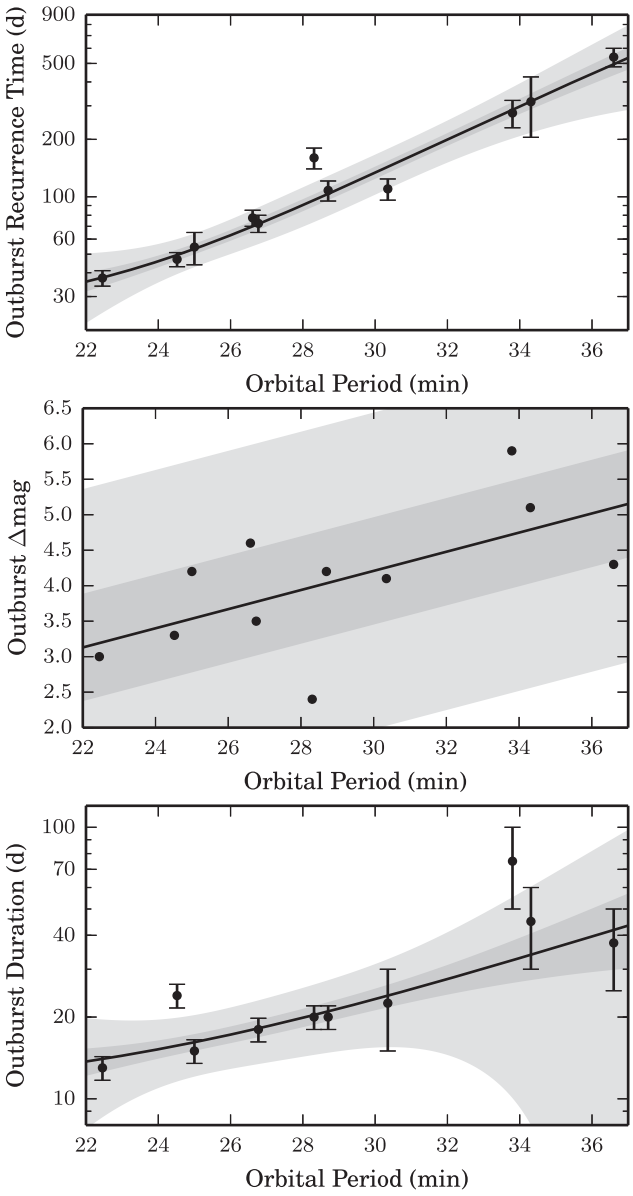

Figure 12. Plots of outburst properties versus orbital period. The solid line is a best-fitting model. For the recurrence time and outburst duration we used a power-law model, while for the outburst magnitude we used a linear model (which corresponds to an exponential model in flux). The former are plotted using a logarithmic scale on the *y*-axis, while we note that magnitudes are already logarithmic. The darker shaded areas represent the 1σ errors while the lighter shaded areas represent the 3σ errors. For the recurrence time and duration, we use the fit errors. For the outburst strength, we use the standard deviation of the residuals. Full details of the fits are given in Appendix A.

that the models for these two properties are too simplistic. However, given the lack of additional data for systems (e.g. component masses), these are likely the best approximations that can be determined at the present time.

4.2.2 Prediction of orbital periods

The measurement of AM CVn system orbital periods is a difficult process, particularly for the faint systems discovered recently. The relation between orbital period and outburst recurrence time presented in Section 4.2 allows us to estimate periods for systems not yet measured. Four systems show multiple outbursts with a consistent recurrence time and have unknown orbital periods. We provide estimated orbital periods for them, along with their outburst properties in Table 4. We caution that these are estimates to serve primarily in observation planning. Errors are derived from a combination of fit parameter errors and outburst recurrence time errors.

4.2.3 Single outburst systems

In Section 3, we separated the outbursting AM CVn systems into those that showed regular outbursts, and those for which only a single outburst has been observed. We also showed in Table 3 that it is highly likely that we missed an outburst for most of the systems. Only for one system did we find a probability of a missed outburst below 50 per cent, while four out of six have missed-outburst probabilities of $\geq$75 per cent.

Before the discovery of a 47 min photometric period in CRTS J0450−0931 (Woudt et al. 2013), only systems with $P_{\rm orb}$ below 40 min were believed to outburst. Even more recently, an outburst in SDSS J0902+3819 – a system with a spectroscopically measured orbital period of 48.3 min (Rau et al. 2010) – was observed in outburst by Kato et al. (2014). While it is not known if all systems with similar orbital periods experience outbursts, the discovery of two systems indicates this is likely not a unique phenomenon.

Using the relation in Section 4.2, the recurrence time for a 38 min system is 2 yr. The recurrence time of a 48 min system according to our relation is 9.6 yr. If we assume our relation holds at such a long orbital period, then even the data presented here do not extend far enough back to contain even two outbursts. The relatively short nature of these outbursts and the faintness of many of the systems makes such detections even more difficult. Only three single-outburst systems were detected in outburst in the PTF data, four systems were detected in 7 yr of CSS data, and one system was detected in 5.5 yr of LINEAR data. For these reasons, we believe that most of the 'single' outburst systems follow the same principles as shorter period orbital systems, but, given their short outburst duration (see Sections 3.2 and 4.1), long recurrence times, and faint quiescent magnitudes, are simply difficult to detect in outburst.

4.3 Implications for discovery of AM CVn systems

The relationships between orbital period and outburst properties developed in Section 4.2 allow us to calculate the detection probability, $p(P_{\rm orb}, m_{\rm qui})$, of an outbursting AM CVn system by a synoptic survey with a known cadence and limiting magnitude. We can use these results to estimate the number of outbursting AM CVn systems with 20 min $< P_{\rm orb} <$ 37 min that a survey could discover. Such a calculation involves two elements. First, we must find the detection probability of an AM CVn system that has a specific orbital period and quiescent magnitude. Secondly, we need a model for the Galactic distribution of AM CVn systems. Here, we calculate the number of systems that could be discovered by two model surveys based on the CSS and the PTF.

4.3.1 Survey definition and system detection probability

We begin by defining our surveys. We assume no weather interruptions, and normal-distributed limiting magnitudes with $\sigma = 0.5$ mag around the median limiting magnitude of the survey. We do not account here for crowding and assume perfect detections (e.g. no

Table 4. Outburst properties of recurring outburst systems with unknown orbital periods.

System	No. of outbursts observed	Observation span (d)	Recurrence time (d)	Duration (d)	Strength (mag)	Est. orbital Per. (min)
PTF1 J2219+3135	9	2726	64 ± 5	<26	4.4	26.1 ± 0.74
SDSS 1043+5632	9	3477	99 ± 12	<55	3.4	28.5 ± 0.92
PTF1 J1632+3511	3	3541	230 ± 35	<80	5.2	32.7 ± 1.1
CRTS J0744+3254	12	3100	239 ± 36	<65	3.8	32.9 ± 1.1

Notes. Definitions of the properties shown here are in Section 2.2. The estimated orbital periods are based on outburst properties and their calculation and accuracy are described in Section 4.2.2. Errors are derived from a combination of the outburst recurrence time error and the fit error. The outburst duration times for all of these systems are upper bounds due to lack of data to find a better estimate.

artefacts). For the CSS-like survey, we assume four exposures per night over 30 min, taken every two weeks (Drake et al. 2009), and a median magnitude of $V = 19.5$. We assume that each field is observed for ∼200 d = 15 observations per year, for 7 yr. For the PTF-like survey, we assume two exposures per night over 1 h, but with a cadence of 4 d and a limiting magnitude of $V = 20.5$. We assume that each field is observed for approximately three months (20 observations) for 3 yr. Lastly, we assume that both surveys cover Galactic latitudes of $15 < b < 90$ at all Galactic longitudes.

We now construct an outburst light-curve model. Although we constructed such a model for the calculation of non-detection probabilities in Section 3.2, that model was only applicable to systems with $P_{\rm orb} > 37$ min. The light-curve profile (see Section 3.1 of this paper and fig. 4 of R12) of outbursting systems with $P_{\rm orb} < 37$ min is substantially different. Thus, we model the outburst as a sudden rise to the outburst magnitude (Δmag + $m_{\rm qui}$, as defined in Section 4.2), and a gradual decline over $t_{\rm dur}$ days to 0.5 mag above $m_{\rm qui}$, with a return to quiescence thereafter.

To calculate the probability, p($P_{\rm orb}$, $m_{\rm qui}$), we use a Monte Carlo approach. For every $P_{\rm orb}$ and $m_{\rm qui}$, we calculate the light curve at the simulated exposure times using a random start time for the outburst sequence. We determine whether a particular light curve was detected based on the criteria in Section 2.2. Briefly, we required at least two consecutive detections (defined as being brighter than the limiting magnitude) within 15 d that were ≥0.5 mag above the quiescence magnitude. We note that we only use the 0.5 mag above quiescence criterion here, as opposed to the 3σ criterion. However, the error of observations at the 5σ limiting magnitude should be ∼0.2 mag, which is consistent with these criteria here. We caution that these criteria for outbursts, and the ones generally applied in this paper, are designed only to ignore fake outbursts. In a real survey, one would also want to select against short outburst-like events, such as M-dwarf flares. We simulate 1000 systems for each $P_{\rm orb}$ and $m_{\rm qui}$. We repeat this process 500 times, and take the mean and standard deviation of the number of systems detected over the number of systems simulated as the detection probability and its associated error. We calculate the detection probability for $20\,{\rm min} \leq P_{\rm orb} \leq 37\,{\rm min}$ in 0.2 min steps and for $17 \leq m_{\rm qui} \leq 26$ in 0.2 mag steps, and interpolate for intermediate values.

In Fig. 13 we show the detection efficiency of our surveys given $P_{\rm orb}$ and $m_{\rm qui}$. We caution that these models do not account for weather and other scheduling irregularities and, particularly in the case of the PTF-like survey, are only vaguely similar to the cadence of the survey they emulate. As expected, longer period systems can be detected to fainter magnitudes given their increased strength, but are not as well detected by the PTF-like survey due to its shorter baseline, relative to the >1 yr recurrence times at these orbital periods. The PTF-like survey is able to detect slightly fainter systems due to being deeper, but the longer baseline of the CSS-like survey removes this advantage.

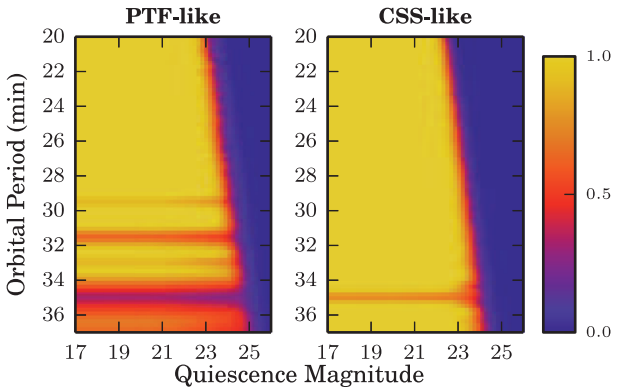

Figure 13. A plot of the detection efficiency of AM CVn systems given an orbital period and quiescent magnitude. A significant decrease in efficiency is seen at $P_{\rm orb} = 35.8$ min, as at this time the recurrence time is about 1 yr. The PTF survey goes slightly deeper, but this is not as large an effect due to the longer baseline of the CSS. The PTF suffers at longer orbital periods as the recurrence times increase to several years.

4.3.2 *System evolution models*

Now that we have $p(P_{\rm orb}, m_{\rm qui})$, we must model the population of AM CVn systems. First, we find the fraction of AM CVn systems at each orbital period. The orbital evolution of AM CVn systems is believed to involve only the effects of gravitational wave radiation and mass transfer (Paczyński 1967; but see Deloye, Bildsten & Nelemans 2005 for a more complex evolutionary model). We assume that the percentage of systems at a given $P_{\rm orb}$ is equal to the amount of time the system spends at that orbital period over the lifespan of the system, which we define to be from $P_{\rm orb} = 5$ to 80 min. This ignores any changes in the birth rates of these systems.

We evolve a system with $M_{\rm acc} = 0.6\,{\rm M}_{\odot}$ and $M_{\rm don} = 0.25\,{\rm M}_{\odot}$ from $P_{\rm orb} = 5$ min to longer orbital periods. The masses are arbitrary, but are in agreement with models and with the measured masses of the components of SDSS J0926+3624 (Copperwheat et al. 2011). To simplify the calculations, we fit these results with a power law and take its derivative, such that $f_{\rm syst}$ is the fractional number of systems per orbital period bin and $P_{\rm orb}$ is in minutes

$$f_{\rm syst}(P_{\rm orb}) = (4.0 \times 10^{-7}) P_{\rm orb}^{2.66}. \quad (1)$$

This equation is normalized, such that $\int_{5\,{\rm min}}^{80\,{\rm min}} f_{\rm syst}(P_{\rm orb})\,{\rm d}P_{\rm orb} = 1$ and hence the integral of $f_{\rm syst}$ between two orbital periods will yield the fraction of a system's lifetime spent between those orbital periods and thus the fraction of known AM CVn systems we expect

to observe between the orbital periods. We note that an analytic derivation of the orbital period derivative, $\dot{P}_{\rm orb}(P_{\rm orb})$, in the limit $M_{\rm don} \ll M_{\rm acc}$ yields $\dot{P}(P_{\rm orb}) \propto P_{\rm orb}^{-8/3}$, consistent with the numerical fit.

We use the same Galactic population distribution model as Nelemans et al. (2001),

$$\rho(P_{\rm orb}, R, z) = \rho_0 f_{\rm syst}(P_{\rm orb}) {\rm e}^{-R/H} {\rm sech}(z/h)^2 \, {\rm pc}^{-3}, \quad (2)$$

where R is the radius from the centre of the Galaxy, z is the distance above the Galactic plane, ρ_0 is the population density at the centre of the Galaxy, H is the scale distance, and h is the scaleheight. We adopt, for the purposes of this calculation, the same scaleheight (300 pc) and scale distance (2.5 kpc) as Roelofs et al. (2007b).

The number of systems with orbital period $P_{\rm orb}$ at a point (r, b, l) when viewed from Earth can then be defined as

$$N_{\rm obs}(P_{\rm orb}, r, b, l) = r^2 \cos(b) \rho(P_{\rm orb}, R, z) {\rm p}(P_{\rm orb}, m_{\rm qui}), \quad (3)$$

where b is the Galactic latitude, l is the Galactic longitude, and we can express R in terms of r, b, and l as $\sqrt{r^2 \cos^2 b + R_{\rm GC}^2 + 2r \cos b \cos l}$. $R_{\rm GC}$ is 8125 pc, the distance from Sun to the Galactic Centre.

We calculate $m_{\rm qui}$ using the distance, r, and the same parametrization for the absolute magnitude as Roelofs et al. (2007b),

$$M_{\rm qui}(P_{\rm orb}) = 10.5 + 0.075(P_{\rm orb} - 30 \, {\rm min}), \quad (4)$$

which is based on fig. 2 of Bildsten et al. (2006). This value for the absolute magnitude is only based on the temperature of the accretor and does not account for any luminosity from the disc. However, the disc has been measured to account for only 30 per cent of an AM CVn system's luminosity (Copperwheat et al. 2011), so this assumption should provide a reasonable estimate.

4.3.3 Simulated survey results

We now combine our model for the detection efficiencies with that for the Galactic distribution to find the number of expected systems with $20 \, {\rm min} \leq P_{\rm orb} \leq 37 \, {\rm min}$ that would be detected by our CSS-like survey and our PTF-like survey. We use the most recent published population density estimate for AM CVn systems from Carter et al. (2013), hereafter C13. Since C13 give the local population density as opposed to the density at the Galactic Centre (where we defined ρ_0), we set $\rho_0 = (5 \pm 3) \times 10^{-7}$ systems ${\rm pc}^{-3} {\rm e}^{{\rm R}\odot \, h^{-1}}$.

We find that over the survey lifetime, our CSS-like survey would detect $(1.76 \pm 1.1) \times 10^{-3}$ systems deg^{-2} or, assuming a total coverage of $\sim$20 000 deg^2, a total of 35 ± 21 systems in total. For our PTF-like survey, we find that it would detect $(1.52 \pm 0.91) \times 10^{-3}$ systems deg^{-2} over the survey lifetime. With a coverage of $\sim$16 000 deg^2, we would expect a total of 24 ± 15 systems. Errors provided are only based on the error provided for the population density estimate.

Have the CSS and the PTF detected as many systems as we would expect if the population densities from C13 are correct? The CSS has detected eight AM CVn systems in outburst with $20 \, {\rm min} < P_{\rm orb} < 37 \, {\rm min}$, and another likely four systems with orbital periods in this range. The PTF has detected six outbursting AM CVn systems in this orbital period range, and an additional three systems with orbital periods likely to be in this range. This indicates that the surveys have detected, respectably, only 34 per cent and 38 per cent of the estimated total, albeit with significant errors in these numbers. This likely shows the value of a dedicated, systematic search for these systems, particularly given the recent results from the partially completed spectroscopic survey of all identified CRTS CVs (Breedt et al. 2014).

We caution that our simulations did not account for several factors. First, we did not account for scheduling irregularities and we assumed a perfect cadence. PTF, in particular, uses variable cadences. A more realistic study of PTF's AM CVn system detection efficiency based on the actual times of exposures is outside the scope of this paper. An additional observational constraint is the difficulty in confirming faint candidates. Systems with quiescent magnitudes significantly fainter than $g' \sim 21$ cannot be spectroscopically confirmed even with 8–10 m class telescopes unless caught in outburst. These factors indicate that while the CSS and the PTF likely contain additional systems, many may be faint and confirming these systems will be extremely difficult.

Although this simulation considers regularly outbursting systems, we also need to consider the probability of detecting longer period systems. If, in fact, longer period systems do outburst as we discuss in Section 4.2.3, and the relation in Section 4.2 (or a similar one) holds even for longer period systems, this implies that systems with orbital periods similar to CRTS J0450−0931 and SDSS J0902+3918 outburst on the decade time-scale. Such a time-scale is not unreasonable, given the behaviour of WZ Sge-type systems. The majority of AM CVn systems are believed to be long-period systems (Nelemans et al. 2001; Nissanke et al. 2012) and faint. Specifically, we can approximate that there are $\sim$2.2 times more AM CVn systems with $37 \, {\rm min} < P_{\rm orb} < 50 \, {\rm min}$ than with $20 \, {\rm min} < P_{\rm orb} < 37 \, {\rm min}$ using our evolutionary model. Yet even if they are bright enough to be visible, only some will outburst during even a decade-long synoptic survey (depending on the actual outburst recurrence time), and of that sample, likely up to 75 per cent (Table 3) will be undetected due to their short outbursts and the relatively sparse coverage of current synoptic surveys.

4.4 Mass transfer rate versus outburst recurrence time

The simplest hypothesis for the increase in outburst recurrence time with increasing orbital period would be that the critical mass needed for the disc instability, $M_{\rm outburst}$, simply takes longer to accumulate as the mass transfer rate decreases. Combining our mass transfer rate model of an AM CVn system developed in Section 4.3.2 with our observed relationship for the outburst recurrence time, $t_{\rm recur}$, in Section 4.2, we find that $M_{\rm outburst} \approx 10^{-10} \, {\rm M}_\odot$ across the large orbital period range. This lends strong support to the hypothesis that the outburst recurrence time is linked to $\dot{M}$. A more sophisticated model could be constructed using Deloye et al. (2005) for $\dot{M}$ and the theory of Kotko et al. (2012) for $M_{\rm outburst}$.

5 CONCLUSIONS AND FURTHER WORK

We have presented light curves of outbursting AM CVn systems drawn from three wide-area synoptic surveys, identified outburst recurrence times for all known outbursting systems with more than one observed outburst, and found relationships between the orbital period and outburst strength, recurrence time, and duration. In particular, the light-curve properties and resulting relationships provide a powerful tool for understanding these and future systems. Although the current DIM has been successful in replicating normal and superoutburst light curves of AM CVn systems (Kotko et al. 2012), the much more diverse behaviour shown here (particularly the sudden changes in outburst behaviour of CR Boo and SDSS J0926+3624) provides additional challenges to the model. The broader set of observations provided by synoptic surveys will

hopefully allow for the better development of AM CVn system outburst models. Lastly, we note that the approach taken here is essentially qualitative in nature. A more rigorous, statistical approach to identifying and measuring outbursts would provide significantly better results, particularly for those systems with few outbursts and/or few observations.

Our attempt to quantify the efficiencies of two different survey models will allow for a better understanding of the potential of future synoptic surveys to identify new AM CVn systems. Confirmation of these efficiencies with data on the actual observation schedules of the surveys will allow a better prediction of how many systems remain in both surveys.

ACKNOWLEDGEMENTS

We thank Lars Bildsten for helpful suggestions related to the recurrence time-orbital period relations. PG and TP thank the Aspen Center for Physics and the NSF Grant #1066293 for hospitality during the preparation of this manuscript. EOO is incumbent of the Arye Dissentshik career development chair and is grateful to support by grants from the Willner Family Leadership Institute Ilan Gluzman (Secaucus NJ), Israeli Ministry of Science, Israel Science Foundation, Minerva, Weizmann-UK and the I-CORE Programme of the Planning and Budgeting Committee and The Israel Science Foundation.

Observations obtained with the Samuel Oschin Telescope at the Palomar Observatory as part of the Palomar Transient Factory project, a scientific collaboration between the California Institute of Technology, Columbia University, Las Cumbres Observatory, the Lawrence Berkeley National Laboratory, the National Energy Research Scientific Computing Center, the University of Oxford, and the Weizmann Institute of Science. The CSS survey is funded by the National Aeronautics and Space Administration under Grant no. NNG05GF22G issued through the Science Mission Directorate Near-Earth Objects Observations Programme. The CRTS survey is supported by the US National Science Foundation under grants AST-0909182. The LINEAR programme is sponsored by the National Aeronautics and Space Administration (NRA no. NNH09ZDA001N, 09-NEOO09-0010) and the USA Air Force under Air Force Contract FA8721-05-C-0002. This research has made use of NASA's Astrophysics Data System.

REFERENCES

Ahn C. P. et al., 2012, ApJS, 203, 21
Anderson S. F. et al., 2005, AJ, 130, 2230
Anderson S. F. et al., 2008, AJ, 135, 2108
Bertin E., Arnouts S., 1996, A&AS, 117, 393
Bildsten L., Townsley D. M., Deloye C. J., Nelemans G., 2006, ApJ, 640, 466
Breedt E., Gänsicke B. T., Marsh T. R., Steeghs D., Drake A. J., Copperwheat C. M., 2012, MNRAS, 425, 2548
Breedt E. et al., 2014, MNRAS, 443, 3174
Carter P. J. et al., 2013, MNRAS, 429, 2143 (C13)
Carter P. J., Steeghs D., Marsh T. R., Kupfer T., Copperwheat C. M., Groot P. J., Nelemans G., 2014a, MNRAS, 437, 2894
Carter P. J. et al., 2014b, MNRAS, 439, 2848
Cenko S. B. et al., 2006, PASP, 118, 1396
Copperwheat C. M. et al., 2011, MNRAS, 410, 1113
Deloye C. J., Bildsten L., Nelemans G., 2005, ApJ, 624, 934
Drake A. J. et al., 2009, ApJ, 696, 870
Efron B., 1982, The Jackknife, the Bootstrap and other Resampling Plans. Society for Industrial and Applied Mathematics, Philadelphia
Espaillat C., Patterson J., Warner B., Woudt P., 2005, PASP, 117, 189
Faulkner J., Flannery B. P., Warner B., 1972, ApJ, 175, L79
Fontaine G. et al., 2011, ApJ, 726, 92
Groot P. J., Nelemans G., Steeghs D., Marsh T. R., 2001, ApJ, 558, L123
Honeycutt R. K., Adams B. R., Turner G. W., Robertson J. W., Ost E. M., Maxwell J. E., 2013, PASP, 125, 126 (H13)
Kato T., Nogami D., Baba H., Hanson G., Poyner G., 2000, MNRAS, 315, 140 (K00)
Kato T. et al., 2001, Inf. Bull. Var. Stars, 5120 (K01)
Kato T., Stubbings R., Monard B., Butterworth N. D., Bolt G., Richards T., 2004, PASJ, 56, 89
Kato T. et al., 2014, PASJ, (doi:10.1093/pasj/psu077)
Kotko I., Lasota J.-P., Dubus G., Hameury J.-M., 2012, A&A, 544, A13
Kupfer T., Groot P. J., Levitan D., Steeghs D., Marsh T. R., Rutten R. G. M., Nelemans G., 2013, MNRAS, 432, 2048
Laher R. R. et al., 2014, PASP, 126, 674
Lasota J.-P., 2001, New Astron. Rev., 45, 449
Law N. M. et al., 2009, PASP, 121, 1395
Levitan D. et al., 2011, ApJ, 739, 68 (L11)
Levitan D. et al., 2013, MNRAS, 430, 996
Levitan D. et al., 2014, ApJ, 785, 114
Margon B., Levitan D., Prince T. A., Hallinan G., 2014, in Woudt P. A., Ribeiro V. A. R. M., eds, ASP Conf. Ser., Stella Novae: Future and Past Decades, preprint (arXiv:1304.4585)
Matthews O. M., Speith R., Wynn G. A., West R. G., 2007, MNRAS, 375, 105
Nather R. E., Robinson E. L., Stover R. J., 1981, ApJ, 244, 269
Nelemans G., 2005, in Hameury J.-M., Lasota J.-P., eds, ASP Conf. Ser. Vol. 330, The Astrophysics of Cataclysmic Variables and Related Objects. Astron. Soc. Pac., San Francisco, p. 27
Nelemans G., Portegies Zwart S. F., Verbunt F., Yungelson L. R., 2001, A&A, 368, 939
Nelemans G., Yungelson L. R., van der Sluys M. V., Tout C. A., 2010, MNRAS, 401, 1347
Nissanke S., Vallisneri M., Nelemans G., Prince T. A., 2012, ApJ, 758, 131
Ofek E. O., Frail D. A., Breslauer B., Kulkarni S. R., Chandra P., Gal-Yam A., Kasliwal M. M., Gehrels N., 2011, ApJ, 740, 65
Ofek E. O. et al., 2012, PASP, 124, 62
Paczyński B., 1967, Acta Astron., 17, 287
Patterson J. et al., 1997, PASP, 109, 1100
Patterson J., Walker S., Kemp J., O'Donoghue D., Bos M., Stubbings R., 2000, PASP, 112, 625
Patterson J. et al., 2002, PASP, 114, 65
Ramsay G. et al., 2010, MNRAS, 407, 1819
Ramsay G., Barclay T., Steeghs D., Wheatley P. J., Hakala P., Kotko I., Rosen S., 2012, MNRAS, 419, 2836 (R12)
Rau A. et al., 2009, PASP, 121, 1334
Rau A., Roelofs G. H. A., Groot P. J., Marsh T. R., Nelemans G., Steeghs D., Salvato M., Kasliwal M. M., 2010, ApJ, 708, 456
Roelofs G. H. A., Groot P. J., Marsh T. R., Steeghs D., Barros S. C. C., Nelemans G., 2005, MNRAS, 361, 487
Roelofs G. H. A., Groot P. J., Marsh T. R., Steeghs D., Nelemans G., 2006a, MNRAS, 365, 1109
Roelofs G. H. A., Groot P. J., Nelemans G., Marsh T. R., Steeghs D., 2006b, MNRAS, 371, 1231
Roelofs G. H. A., Groot P. J., Nelemans G., Marsh T. R., Steeghs D., 2007a, MNRAS, 379, 176
Roelofs G. H. A., Nelemans G., Groot P. J., 2007b, MNRAS, 382, 685
Roelofs G. H. A., Groot P. J., Steeghs D., Marsh T. R., Nelemans G., 2007c, MNRAS, 382, 1643
Roelofs G. H. A. et al., 2009, MNRAS, 394, 367
Roelofs G. H. A., Rau A., Marsh T. R., Steeghs D., Groot P. J., Nelemans G., 2010, ApJ, 711, L138
Ruiz M. T., Rojo P. M., Garay G., Maza J., 2001, ApJ, 552, 679
Sagiv I. et al., 2014, AJ, 147, 79
Scargle J. D., 1982, ApJ, 263, 835
Sesar B., Stuart J. S., Ivezić Ž., Morgan D. P., Becker A. C., Woźniak P., 2011, AJ, 142, 190

Shapiro S. S., Wilk M. B., 1965, Biometrika, 52, 591
Shears J., Brady S., Koff R., Goff W., Boyd D., 2011, preprint (arXiv:1104.0107)
Solheim J., 2010, PASP, 122, 1133
Steeghs D., Marsh T. R., Barros S. C. C., Nelemans G., Groot P. J., Roelofs G. H. A., Ramsay G., Cropper M., 2006, ApJ, 649, 382
Stokes G. H., Evans J. B., Viggh H. E. M., Shelly F. C., Pearce E. C., 2000, Icarus, 148, 21
Tsugawa M., Osaki Y., 1997, PASJ, 49, 75
Warner B., 1995, Cataclysmic Variable Stars. Cambridge Univ. Press, Cambridge
Wheatley J. M., Welsh B. Y., Browne S. E., 2008, AJ, 136, 259
Woudt P. A., Warner B., Rykoff E., 2005, IAU Circ., 8531, 3
Woudt P. A., Warner B., Motsoaledi M., 2013, Astron. Telegram, 4726, 1

APPENDIX A: SYSTEM MODEL FITTING DETAILS

A1 Outburst recurrence time and duration fits

In Section 4.2 and Fig. 12, we provided relationships between system properties and orbital period based on a fit to a model. In particular, we fitted the known values for outburst recurrence time and outburst duration time to a power-law model (outburst Δmag was fitted to a linear model and is described in Appendix A2),

$$y = \alpha P_{\rm orb}^{\beta} + \gamma,$$

where y is the property of the outburst, $P_{\rm orb}$ is the orbital period in minutes, and α, β, and γ are fit parameters.

To fit our observed values for the outburst properties, we used the NONLINEARMODELFIT function in Wolfram Research's Mathematica 9.0. The errors used for recurrence times are given in Table 2. For outburst duration, we assumed a 10 per cent error for all systems that do not have an upper limit in Table 2. For those with upper limits, we assumed that the duration was 75 per cent of the upper limit, with a 25 per cent error. These choices are somewhat arbitrary, but are reasonable given the light curves.

Recurrence time fit errors. The best-fitting values for the recurrence time are $\alpha = 1.53 \times 10^{-9}$, $\beta = 7.35$, and $\gamma = 24.7$. The elements of covariance matrix for the parameters are $\Sigma_{\alpha\alpha} = 1.62 \times 10^{-17}$, $\Sigma_{\beta\beta} = 0.567$, $\Sigma_{\gamma\gamma} = 39.5$, $\Sigma_{\alpha\beta} = -3.03 \times 10^{-9}$, $\Sigma_{\alpha\gamma} = -2.22 \times 10^{-8}$, and $\Sigma_{\beta\gamma} = 4.09$.

Outdurst duration fit errors. The best-fitting values for the recurrence time are $\alpha = 0.390$, $\beta = 0.122$, and $\gamma = 7.90$. The elements of covariance matrix for the parameters are $\Sigma_{\alpha\alpha} = 4.80 \times 10^{-10}$, $\Sigma_{\beta\beta} = 5.99$, $\Sigma_{\gamma\gamma} = 19.5$, $\Sigma_{\alpha\beta} = -5.36 \times 10^{-5}$, $\Sigma_{\alpha\gamma} = -9.08 \times 10^{-5}$, and $\Sigma_{\beta\gamma} = 10.1$.

Model choice. We fit both the power-law model described here and an exponential model. We then calculated the F-ratio (defined as the ratio of the sum of the squares of the residuals) and found the p-value for this ratio. Additionally, we performed the χ^2 test on each model. We caution that both of these tests may provide erroneous values given the small number of samples.

For the recurrence time, the exponential model was favoured with a p-value of 0.4. The χ^2 value for this model was also slightly lower than for the power-law model (53.5 versus 56.2). Both of these differences are small. For the duration, neither model was favoured by the F-ratio and there was a difference of 0.7 in the χ^2 values. Given the results from this test, the possible impact of the small number of samples, and our preference for a power-law model given the orbital evolution equation, we chose the power-law model.

A2 Outburst strength fit

For the outburst strength, we fit a linear model,

$$\Delta\text{mag} = \alpha P_{\rm orb} + \beta,$$

using the LINEARMODELFIT function in Wolfram Research's Mathematica 9.0. We did not provide any weights as there is no good method of obtaining meaningful estimates of our errors. We found a best fit of $\alpha = 0.13$ and $\beta = 0.16$. Errors are estimated calculating the standard deviation of the residuals from the model, with $\sigma = 0.74$ mag.

This paper has been typeset from a TEX/LATEX file prepared by the author.